

**PHYSICAL AND CHEMICAL PERFORMANCE OF VANADYL
PYROPHOSPHATE CATALYSTS OBTAINED VIA DIFFERENT
CALCINATION DURATIONS**

TAN LING HAN

**A project report submitted in partial fulfilment of the
requirements for the award of the degree of
Bachelor of Engineering(Hons.) Chemical Engineering**

**Faculty of Engineering and Science
Universiti Tunku Abdul Rahman**

April 2011

DECLARATION

I hereby declare that this project report is based on my original work except for citations and quotations which have been duly acknowledged. I also declare that it has not been previously and concurrently submitted for any other degree or award at UTAR or other institutions.

Signature : _____

Name : Tan Ling Han

ID No. : 07 UEB 06703

Date : 15th of April, 2011

APPROVAL FOR SUBMISSION

I certify that this project report entitled **“PHYSICAL AND CHEMICAL PERFORMANCE OF VANADYL PYROPHOSPHATE CATALYSTS OBTAINED VIA DIFFERENT CALCINATION DURATIONS”** was prepared by **TAN LING HAN** has met the required standard for submission in partial fulfilment of the requirements for the award of Bachelor of Engineering(Hons.) Chemical Engineering at Universiti Tunku Abdul Rahman.

Approved by,

Signature : _____

Supervisor : Dr. Leong Loong Kong

Date : _____

The copyright of this report belongs to the author under the terms of the copyright Act 1987 as qualified by Intellectual Property Policy of University Tunku Abdul Rahman. Due acknowledgement shall always be made of the use of any material contained in, or derived from, this report.

© 2011, TAN LING HAN. All right reserved.

ACKNOWLEDGEMENTS

I would like to thank everyone who had contributed to the successful completion of this project. I would like to express my gratitude to my research supervisor, Dr. Leong Loong Kong for his invaluable advice, guidance and his enormous patience throughout the development of the research.

In addition, I would also like to express my heartiest gratitude to my loving parents. They have given me unconditional support and encouragement, beginning from involving and conducting all the laboratory work and producing this technical report.

I would like to thank Ms. Catherine Loh, Ms. Zoey Kang and Mr. Max for guidance and help in conducting the laboratory work as well as my fellow course mates who have provided necessarily materials to aid in my writing and shared points with me whilst discussing the content of the essay. This report would not be possible without their help. Lastly, my heartiest appreciation goes to my personal friend who has helped me to proof read and provide constructive comments to help me improve better.

**PHYSICAL AND CHEMICAL PERFORMANCE OF VANADYL
PYROPHOSPHATE CATALYSIS OBTAINED VIA DIFFERENT
CALCINATION DURATIONS**

ABSTRACT

Catalysis, being the workhorse of the chemical industries nowadays, it contributes a crucial role in the development of new products. Maleic anhydride (MA) is a versatile chemical compound which is commonly used in the production of unsaturated polyester resins, lube oil additives, alkyl resins, and etc. Catalysis plays an important role in the production of MA in order to meet the demanding market. Selective oxidation of *n*-butane over vanadyl pyrophosphate (VPO) as the catalyst in the reaction results in the formation of MA. The VPO catalyst was synthesized through sesquihydrate precursor route. Several physico-chemical techniques were used in investigating the sample, namely X-ray Diffraction (XRD), BET single point surface area, redox titration, Inductively-Coupled Plasma- Optical Emission Spectrometer (ICP-OES) and finally Scanning Electron Microscopy with Energy Dispersive X-ray spectrometer (SEM-EDX). Catalysts were found to exhibit good crystalline with characteristic peaks of vanadyl pyrophosphate phase. The VPO catalyst obtained via 3 days calcination possessed the highest surface area (22.525 m²/g). Catalysts resulted in a plate-like crystal formed in the rosebud agglomerates. Redox titration indicates that V⁵⁺ phase exists in the catalysts but the correlation between the average oxidation number and calcination durations could not be established. Finally, the P/V ratios obtained via ICP- OES lie closely to ratio of 1.0 and they are in close agreement with P/V ratios obtained via EDX.

TABLE OF CONTENTS

DECLARATION	ii
APPROVAL FOR SUBMISSION	iii
ACKNOWLEDGEMENTS	v
ABSTRACT	vi
TABLE OF CONTENTS	vii
LIST OF TABLES	x
LIST OF FIGURES	xi
LIST OF SYMBOLS / ABBREVIATIONS	xii
LIST OF APPENDICES	xiii

CHAPTER

1	INTRODUCTION	1
1.1	Catalysis and Catalysts	1
1.2	Types of Catalysis	3
1.2.1	Homogeneous Catalysis	3
1.2.2	Heterogeneous Catalysis	4
1.3	Energy Profiles of Reaction with Catalysts	5
1.4	Essential Properties of Good Catalysts	7
1.5	Importance and Uses of Catalysts	8
1.6	Problem Statements	9
1.7	Objectives of Research	11
2	LITERATURE REVIEW	12
2.1	Vanadyl Pyrophosphate Catalyst (VO) ₂ P ₂ O ₇	12

2.2	Preparation of Vanadium Phosphorus Oxide Catalyst	13
2.2.1	Aqueous Medium	13
2.2.2	Organic Medium	14
2.2.3	Dihydrate Precursor Route	15
2.2.4	Hemihydrate Precursor Route	15
2.2.5	Sesquihydrate Precursor Route	16
2.3	Parameters of Vanadium Phosphorus Oxide Catalyst	17
2.3.1	Parameter: Calcination Condition	18
2.3.2	Parameter: Support System	18
2.3.3	Parameter: Dopant	19
2.4	Maleic Anhydride	19
2.4.1	Uses of Maleic Anhydride	20
2.4.2	Oxidation of <i>n</i> -butane to Maleic Anhydride	21
3	METHODOLOGY AND CHARACTERISATION TECHNIQUES	23
3.1	Materials and Gases used	23
3.2	Methodology	24
3.2.1	Preparation of the Vanadyl Phosphate Dihydrate	24
3.2.2	Preparation of Vanadium Phosphorus Oxide Catalysts	26
3.3	Characterisation Techniques and Instrumentations	28
3.3.1	X-Ray Diffraction (XRD) Analysis	28
3.3.2	BET Surface Area Measurements	30
3.3.3	Redox Titration	32
3.3.4	Scanning Electron Microscopy with Energy Dispersive X-ray Spectrometer (SEM-EDX)	33
3.3.5	Inductively-Coupled Plasma- Optical Emission Spectroscopy (ICP-OES)	35
4	RESULTS AND DISCUSSION	36
4.1	Introduction	36
4.2	X-Ray Diffraction (XRD)	37

4.3	Brunauer-Emmer-Teller Single Point Surface Area (BET)	38
4.4	Scanning Electron Microscopy (SEM)	39
4.5	Redox Titration	42
4.6	Inductively- Coupled Plasma- Optical Emission Spectrometer (ICP-OES)	42
4.7	Energy Dispersive X-Ray Diffraction (EDX)	43
5	CONCLUSION AND RECOMMENDATIONS	44
5.1	Conclusions	44
5.2	Recommendations	44
	REFERENCES	45
	APPENDICES	47

LIST OF TABLES

TABLE	TITLE	PAGE
1.1	Examples of Catalyst	2
1.2	Types of Porous Catalyst	7
2.1	Uses of Maleic Anhydride in year 2000	21
3.1	The range of calibration standards used in the ICP-OES	35
4.1	Particles' size of each plane for each sample	38
4.2	BET Surface Area for each sample	38
4.3	V _{AVERAGE} for each sample obtained	42
4.4	P/V atomic ratio	43
4.5	P/V atomic ratio	43

LIST OF FIGURES

FIGURE	TITLE	PAGE
1.1	Steps in a Heterogeneous Catalytic Reaction	5
1.2	Steps in a Heterogeneous Catalytic Reaction	6
1.3	World Consumption of Maleic Anhydride in year 2008	10
3.1	Diagrams show the preparation steps of the $\text{VOPO}_4 \cdot 2\text{H}_2\text{O}$	25
3.2	Diagrams show the preparation steps of the $(\text{VO})_2\text{P}_2\text{O}_7$	27
3.3	X-rays scattered by atom in an ordered lattice interfere	29
3.4	Shimadzu diffractometer model XRD-6000	30
3.5	Thermo Finnigan Sorptometric 1990	31
3.6	Diagram shows the experiment of Redox Titration	33
3.7	Hitachi S-3400N	34
3.8	Perkin- Elmer Emission Spectrometer Model Plasma 1000	35
4.1	XRD Profiles for Different Calcination Duration	37
4.2	SEM Image of VPO24	40
4.3	SEM Image of VPO48	40
4.4	SEM Image of VPO72	41
4.5	SEM Image of VPO96	41

LIST OF SYMBOLS / ABBREVIATIONS

t	Crystallite size for ($h\ k\ l$) phase
λ	X-ray wavelength of radiation for CuK α
FWHM	Full width at half maximum
K	Kelvin
N ₂	Nitrogen gas
H ₂	Hydrogen gas
NO _x	Nitrogenous gas
CO ₂	Carbon Dioxide
MA	Maleic Anhydride
VPO	Vanadyl Pyrophosphate
BET	Brunauer-Emmett-Teller
XRD	X-Ray Diffractometer
SEM-EDX	Scanning Electron Microscopy incorporated with Energy Dispersive X-Ray Diffraction
ICP-OES	Inductively- Coupled Plasma- Optical Emission Spectrometer
SiO ₂	Silicon Dioxide
TiO ₂	Titanium Dioxide
Al ₂ O ₃	Aluminium Oxide
SiC	Silicon Carbide
VPO24	VPO Catalyst under 24 hour calcination
VPO48	VPO Catalyst under 48 hour calcination
VPO72	VPO Catalyst under 72 hour calcination
VPO96	VPO Catalyst under 96 hour calcination

LIST OF APPENDICES

APPENDIX	TITLE	PAGE
A	Volume of Isobutanol Used	47
B	Volume of Distilled Water Used	49
C	Crystallite Size Measurements by using Powder XRD Technique	49
D	Preparation of Diphenylamine, Ph ₂ NH Indicator (Redox Titration)	49
E	Preparation of 2 M Sulphuric Acid, H ₂ SO ₄ Solution	50
F	Preparation of 0.1 M Sulphuric Acid, H ₂ SO ₄ Solution	51
G	Preparation of 0.01 M Potassium Permanganate, KMnO ₄ (Redox Titration)	51
H	Preparation of 0.01 M Ammonium Iron(II) Sulphate, (NH ₄) ₂ Fe(SO ₄) ₂ ·6H ₂ O (Redox Titration)	52
I	Oxidation State of Vanadium (Redox Titration)	53

CHAPTER 1

INTRODUCTION

1.1 Catalysis and Catalysts

In today's chemical industries, catalysis does contribute a vital role to most of the newly developed commercial products. A catalytic reaction involves several complications such as the possible changes in the catalyst during the reaction as well as the interaction between the reaction species and the solid catalyst. Not to mention there are usually a few reactive species involved in the reaction. As can be seen from here, the production could be enhanced and optimized with a good foundation of the mechanism held behind the heterogeneous reaction system. (Fogler, 2006)

In general, catalysis is primarily defined as the study, occurrence and uses of catalysts and the catalytic processes. Catalysis can be categorised into two major types, namely homogeneous process and heterogeneous process, which will be further described in section 1.2. However, there is another type of catalysis which termed biocatalysis. (Chorkendorff and Niemantsverdriet, 2003)

As the name implies, the biocatalysis concerns about the biological reaction occur in human body or organism. The catalyst employed in biocatalysis is known as enzyme, which is usually a large protein. Enzymes allow biological reactions to occur at a rate necessary to maintain life, such as building up of proteins or DNA, or the decomposition of larger molecules into smaller one. Some examples of the enzyme are protease, amylase and lipase. (Chorkendorff and Niemantsverdriet, 2003)

In terms of homogeneous and heterogeneous processes, catalyst is known as a chemical substance that could accelerate the rate of the particular reaction, either forward to reverse order to the same extent. A catalyst offers a more complex, but energetically much more favourable route for the non-catalytic reaction. With this, the process could be carried out under industrially feasible conditions of pressure and temperatures. (Chorkendorff and Niemantsverdriet, 2003)

Catalysts affect the rate of a chemical reaction, but emerge from the process unchanged. Thus, the catalysts are reusable for the next cycle of the reaction provided that they have not been deactivated. In addition, the overall change of the free energy of the catalytic process and uncatalysed process are the same. This indicates that catalyst does not affect the equilibrium of the reaction. On the other word, catalysts affect the kinetic of the reaction, but not the thermodynamics. Table 1.1 shows some of the catalysts which are used in the industry. (Fogler, 2006)

Table 1.1: Examples of Catalyst

Reaction	Catalyst
Decomposition of hydrogen peroxide	Manganese (IV) oxide, MnO_2
Nitration of benzene	Concentrated sulphuric acid
Manufacture of ammonia by Haber process	Iron
Hydrogenation of a C=C double bond	Nickel

1.2 Types of Catalysis

The two major types of catalytic processes are homogeneous and heterogeneous processes. (Fogler, 2006)

1.2.1 Homogeneous Catalysis

Process in which it involves both catalyst and reactant in the same phase is termed homogeneous catalysis due to the uniformity of the phase in which it occurs. Usually gas phase is observed in homogeneous process. A typical example of homogeneous catalysis is the decomposition of the ozone in atmosphere via the reaction with chlorine atom. Another common example is the industrial Oxo process for manufacturing normal isobutylaldehyde. (Fogler, 2006)

Homogeneous catalysis has several advantages over heterogeneous catalysis: (Bartholomew and Farrauto, 2005)

- Homogeneous catalysis is more active and/ or selective in a number of reactions. This is because the homogeneous catalyst can have multiple valence states, can form both ionic and covalent bonds and can assume a variety of geometric structure, i.e. planar, octahedral, trigonal, etc. (Halpern, 1987). Because of its high catalyst selectivity, the process could be carried out under a milder condition such as lower temperature or pressure.
- Their mechanisms are practically easier to characterized and manipulated to optimize a process.
- Newly developed or enhanced homogeneous catalytic processes are, in general, much easier to transfer to industrial practice than heterogeneous processes (Cornils, 2003). In other words, homogeneous catalysts processes are much easier to scale up than heterogeneous processes due to the absence of mass transfer resistances and the inherent similarity between lab and industrial conditions; this is especially true for catalysts developed or modified by combinatorial (high-throughput) methods.

The principle disadvantages are

- Relatively low productivity
- Fragility (thermal instability), which limits their application to relatively mild conditions

The difficulty encountered in separating the solid catalyst from the products, medium and unconverted reactants.

1.2.2 Heterogeneous Catalysis

A heterogeneous reaction involves more than one phase. Usually the catalyst would be in solid form, and the reactants would be in gas or liquid phase. Comparatively, heterogeneous is more common seen in industries. This is due to the simple and complete separation of the fluid product mixture from the surface of the solid catalyst possessed heterogeneous catalysis. This feature has made heterogeneous catalysis favourable as the solid catalyst is relatively expensive and the reuse is demanded. Besides, heterogeneous reaction usually occurs at very near the fluid-solid interface. (Fogler, 2006)

A heterogeneous catalytic reaction involves seven steps: (Fogler, 2006)

1. Mass transfer (diffusion) of the reactant(s) (e.g., species A) from the bulk fluid to the external surface of the catalyst pellet.
2. Diffusion of the reactant from the pore mouth through the catalyst pores to the immediate vicinity of the internal catalytic surface.
3. Adsorption of reactant A onto the catalyst surface.
4. Reaction on the surface of the catalyst (e.g., $A \rightarrow B$)
5. Desorption of the products (e.g., B) from the surface.
6. Diffusion of the products from the interior of the pellet to the pore mouth at the external surface.
7. Mass transfer of the products from the external pellet surface to the bulk fluid.

The seven steps in a heterogeneous catalytic reaction are depicted schematically in the Figure 1.1:

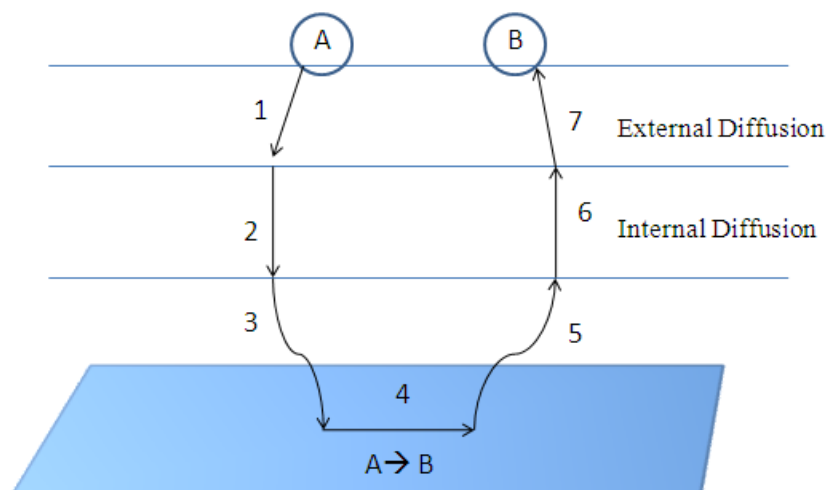


Figure 1.1: Steps in a Heterogeneous Catalytic Reaction

1.3 Energy Profiles of Reaction with Catalysts

As mentioned above, catalysts offer the reaction to be carried out with an energetically much more favourable route. Commercial chemical catalysts are very important. Approximately one third of the material gross national product of the United States involves a catalytic process somewhere between raw materials and finished product. In order to meet the market demand, the chemical industry is in dire need to invent new ways to increase the product yield and selectivity from chemical reactions. The development and use of catalysts plays the dominant part of the constant research. With the different pathway of lower activation energy barrier, both the yield and selectivity can be affected. (Chorkendorff and Niemantsverdriet, 2003)

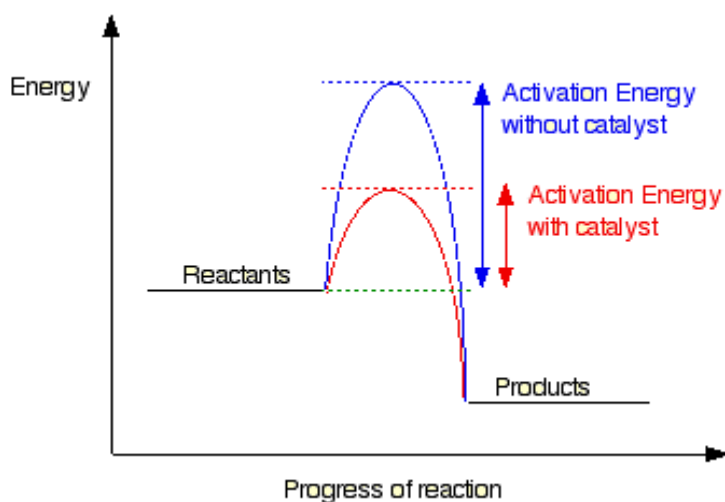


Figure 1.2: Steps in a Heterogeneous Catalytic Reaction

(Source : <http://www.chemguide.co.uk/physical/basicrates/catalyst.html>)

From the figure above, it can be concluded that the activation energy without catalyst is much higher than the one with catalyst.

For a chemical reaction to occur, collision among reactants is required. The higher the collision, the higher is the reaction rate. However, for collision to occur, the molecules of the reactant must come across certain energy barrier possessed. Only molecules with substantial energy could pass the barrier and thus form products. This also explains why the rate of chemical reaction is higher when the temperature rises. The heat is supplied and converted into the internal energy of the molecules. (Chorkendorff and Niemantsverdriet, 2003)

Nonetheless, not every chemical reaction requires high temperature, or other physical conditions to be altered. Sometimes the conditions are difficult to be achieved industrially. For example, the conversion of N_2 and H_2 into ammonia is practically impossible above $600\text{ }^{\circ}\text{C}$. In this case, higher temperatures are needed to break the very strong $N\equiv N$ bond in N_2 . Without catalysts, many reaction that are common in chemical industry would not be possible, and many other processes would not be economical. (Fogler, 2006)

Catalysts could overcome the problems encountered by providing a different molecular path for the reactants to react. It does not lower the original energy barrier,

but provide a route with lower energy barrier. Hence, the probability for molecules of substantial energy to collide with each other increases, which results in high productivity of the desirable products. (Fogler, 2006)

1.4 Essential Properties of Good Catalysts

Catalysts are known to accelerate the rate of the chemical reaction. Important physical properties of catalysts include the particle size and shape, surface area, pore volume, pore size distribution, and strength to resist crushing and abrasion. (Chorkendorff and Niemantsverdriet, 2003)

Since a catalytic reaction occurs at the fluid-solid interface, a large interfacial area is almost always essential in attaining a significant reaction rate. In many catalysts, this area is provided by an inner porous structure (i.e., the solid contains many fine pores, and the surface of these pores supplies the area needed for the high rate of reaction). Catalysts which are classified according to the pores' diameter are as followed: (Bartholomew and Farrauto, 2005)

Table 1.2: Types of Porous Catalyst

Microporous	Mesoporous	Macroporous
Less than 2 nm	In the range of 2 to 50 nm	More than 50 nm

The surface area possessed by a catalyst could be determined from the amount of nitrogen physically absorbed onto the surface of the catalyst. Physical adsorption is similar to condensation. It is exothermic and the heat of adsorption is relatively small. The molecules of nitrogen interact with the surface and multilayers form. The nitrogen adsorption data is interpreted with BET (Brunauer, Emmett, Teller) model. (Bartholomew and Farrauto, 2005)

On the other hand, pore volumes and pore size distribution do affect the performance of the catalyst. The pore volumes could be determined by measurements of desorption nitrogen from the catalyst. The principle held behind

this technique is the capillary condensation that occurs in small pores at pressure lower than the vapour pressure of the adsorbed nitrogen. Smaller diameter of the pore leads to lower vapour pressure of liquid in it. (Bartholomew and Farrauto, 2005)

Besides, the pore size distribution could be obtained by mercury penetration. This technique uses mercury to be forced into the pores on the surface of the catalyst under pressure of approximately 700 atm. The mercury that applied under this pressure is required to fill a pore with a diameter of about 10 nm. The amount of uptake as a function of pressure determines the pore size distribution of the larger pores. (Bartholomew and Farrauto, 2005)

1.5 Importance and Uses of Catalysts

Catalysis is indispensable in the modern technological society. In fact, the world wide economy is greatly dependent on the catalytic production of chemicals and fuels. In today's economy, the four largest sectors comprise petroleum, power, chemicals and food industries. These four major sectors are accountable for more than 10 trillion dollars of gross world product, which are greatly associated with catalytic processes for optimum productivity. (Chorkendorff and Niemantsverdriet, 2003)

The generations of energy, fuels and chemicals from natural gas, coal and biomass involve a lot of catalytic processes. Due to the petroleum scarcity, natural gas and coal are replacing it as the major source of energy and chemicals gradually. As constrained by the environmental impact and the petroleum scarcity issues, renewable energy are extremely important. Hence, the catalytic reactions are essential in the process for converting the biomass to fuels and chemicals. (Chorkendorff and Niemantsverdriet, 2003)

Besides, the other industrial area which involves catalysis is environmental engineering. Nowadays, the destructions caused by humankind are getting more and more attention from everyone. Pollutions caused by the wastes produced from the

industrial processes require immediate action to prevent the environmental conditions from deteriorating. Once again, catalysis is brought into consideration in the effort of improving the environment quality. (Chorkendorff and Niemantsverdriet, 2003)

With catalysis being employed in auto/ truck emissions control, it could minimize the start-up emission, NO_x reduction traps for lean-burn or diesel engines, and the selective catalytic converters (SCR) for reducing NO_x in diesel truck engines. Considering the role contributed by catalysis in restoring the environmental conditions in long run, there will be some catalysis based converters to convert the undesirable gases such as carbon monoxide and carbon dioxide to useful fuels and other chemicals as well as new catalytic processes to minimize hydrocarbons and CO₂ emissions. (Chorkendorff and Niemantsverdriet, 2003)

In addition, catalysis is fundamental to life. The biological reactions in our body are catalyzed by enzyme, as denoted earlier as nature's catalysts. Biological processes such as respiration have to occur rapidly at ambient temperatures and pressures so that the materials in our body can survive. Most of the life-related reactions are enzymatic. (Chorkendorff and Niemantsverdriet, 2003)

In conclusion, catalysis plays an important role in sustaining our life and satisfying the demanded market in all aspects.

1.6 Problem Statements

Initially, the chemical industry was employing alkenes and mono-olefins as the structure-directing agent. However, due to the price and environmental effects caused by these chemicals, the industry is now in transition from employing alkenes and mono-olefins to alkane as the core materials. Alkane is relatively cheap and readily available. Moreover, it possesses less environmental impacts. The selectively oxidation to produce maleic anhydride (MA) was the only process which was successfully carried out using alkane. (Xue, Zhi-yang, 1999)

Before the 1980s, vapor-phase oxidation of benzene over vanadium-based catalyst was the dominant technique for producing MA. The discovery of the high selectivity VPO has enabled the direct oxidation of *n*-butane to MA to be practiced by the industry. Since the mid-1980s, all North American producers have used this *n*-butane oxidation process to produce MA. Its current capacity in the U.S. is 450 million-lb per year. Figure 1.3 depicts the world consumption of MA in year 2008. (Xue, Zhi-yang, 1999)

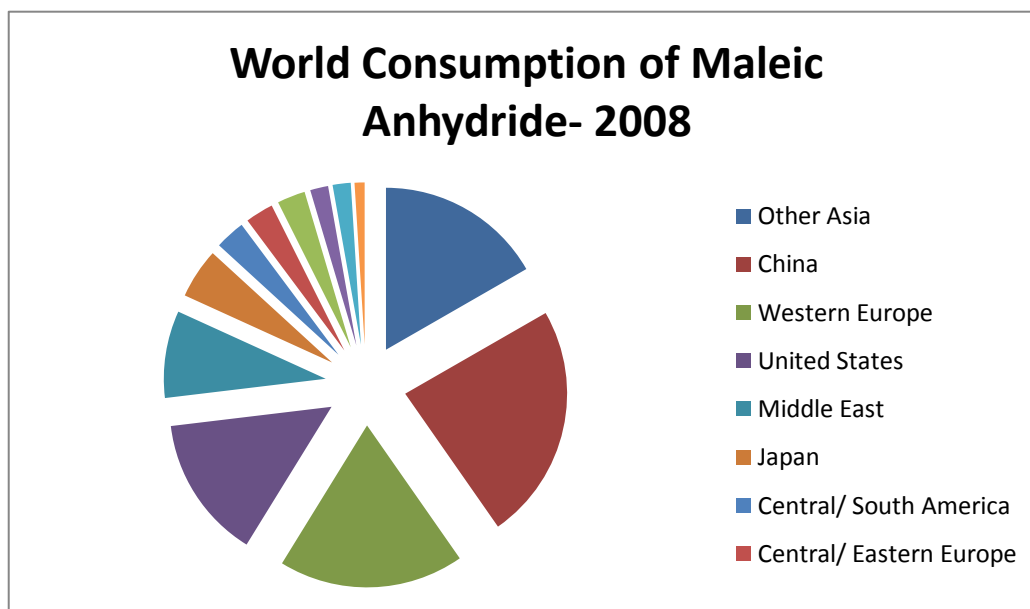


Figure 1.3: World Consumption of Maleic Anhydride in year 2008
(Source: <http://www.sriconsulting.com/CEH/Public/Reports/672.5000/>)

However, the selectivity and activity of the VPO catalyst has not been optimized yet. According to the senior manager of process optimization department from BASF PETRONAS, the selectivity and activity of the VPO catalyst are approximately 82 % and 65 %, respectively. (Albert Su, 2010)

In order to meet the demand of MA, the improvement of the physical and chemical performance of VPO catalyst for selective oxidation of *n*-butane to MA is desirable. This technical report focuses on the effect of calcination durations of the precursor, vanadyl (IV) hydrogen phosphate sesquihydrate, $\text{VOHPO}_4 \cdot 1.5\text{H}_2\text{O}$. The calcinations were carried out at different durations, ranging from 24 hours to 96 hours. The calcination durations of VPO catalyst was manipulated in the hope to achieve higher selectivity and activity.

1.7 Objectives of Research

- i. To synthesize the VPO catalysts via sesquihydrate route.
- ii. To investigate the effect of calcination durations towards the physical and chemical properties of VPO catalysts.

CHAPTER 2

LITERATURE REVIEW

2.1 Vanadyl Pyrophosphate Catalyst $(VO)_2P_2O_7$

Vanadyl pyrophosphate (VPO) is the unique catalyst used in the partial oxidation of *n*-butane to produce maleic anhydride (MA). The VPO catalyst is prepared via a multistep transformation from the precursor $VOHPO_4 \cdot 0.5H_2O$. The activated VPO catalyst is known to have a complicated micro-structure often composed of numerous crystalline phases and some amorphous phases. The major crystalline phase is vanadyl pyrophosphate $((VO)_2P_2O_7)$. A second phase such as $VOPO_4$ could be detected during the pretreatment and the reaction. The identified $VOPO_4$ phases are α , α_{II} , β , γ , δ - $VOPO_4$. $VO(PO_3)_2$ is another detectable crystalline phase in the VPO catalyst. (Gulianti and Carreon, 2005)

The characteristics of VPO have been taken into consideration as it could accelerate the rate of the chemical reaction and thus increase the production of MA. The VPO catalysts are generated by thermal dehydration of its precursor, vanadyl (IV) hydrogen phosphate hemihydrates, $VOHPO_4 \cdot 0.5H_2O$. In addition, VPO catalyst requires no support in the partial oxidation of *n*-butane. This feature has made the catalyst more favourable. Nonetheless, the catalytic activity shown by the VPO catalyst is dependent on several criteria, namely: (Gulianti and Carreon, 2005)

- i. The method of $VOHPO_4 \cdot 0.5H_2O$ synthesis (types and concentrations of reagents, reducing agents and solvents, the reduction temperature and synthesis duration)

- ii. The procedures for activation and conditioning of the precursor at high temperature
- iii. The nature of the metal promoters

These factors can be manipulated while generating the VPO catalyst and the physical, chemical and catalytic performance can be examined in order to determine the appropriate conditions for the optimum performance of VPO catalyst. However, in this report, the variable that is being manipulated is the calcination durations of the precursor, vanadyl (IV) hydrogen phosphate hemihydrates, $\text{VOHPO}_4 \cdot 0.5\text{H}_2\text{O}$. (Taufiq-Yap *et al.*, 2001)

2.2 Preparation of Vanadium Phosphorus Oxide Catalyst

The vanadium phosphorus oxide catalyst could be prepared in different medium and several routes, namely aqueous medium, organic medium, dihydrate precursor route, hemihydrate precursor route and finally, sesquihydrate precursor route. In this technical report, the method employed in preparing the vanadium phosphorus oxide catalyst is sesquihydrate precursor route.

2.2.1 Aqueous Medium

With different preparation route, the catalyst's crystallites give different morphology due to different reducing agent used. The reducing agent used in aqueous medium is a mineral agent in water with phosphoric acid. The preparation work for vanadium phosphorus oxide catalyst in aqueous medium could be conducted as followed: (Centi *et al.*, 1993)

1. 15 g of V_2O_5 (σ) was dissolved in 200 ml of 37 % HCl.
2. The solution was refluxed and stirred until complete reduction to vanadium (IV). This step takes about three hours.
3. 85 % of *ortho*-phosphorus acid ($o\text{-H}_3\text{PO}_4$) was added to obtain the desired P/V atomic ratio.

4. This solution was allowed to boil for 2 hours and concentrated to a volume of 20 mL to which hot water was then added to obtain blue vanadyl *ortho*-phosphate.
5. After evaporation, the solid obtained, which is known as the precursor, was dried at 423 K overnight.

Calcination was then performed in air at 673 K with a flow of mixture which comprises 0.75 % *n*-butane and air for 18 hours and allowed to cool down for four hours.

2.2.2 Organic Medium

In organic medium, the reducing agent used is an organic medium such as methanol or isobutanol prior to the addition of phosphoric acid. Organic medium produces higher specific surface area than aqueous medium due to the nature of the alcohol. (Ellison *et al.*, 1994)

The preparation work for vanadium phosphorus oxide catalyst in organic medium could be conducted as followed: (Centi *et al.*, 1993)

1. Vanadium pentoxide, V_2O_5 (15.0 g from Fluka), was suspended by rapid stirring into a mixture of isobutyl alcohol (90 cm^3) and benzyl alcohol (60 cm^3).
2. The vanadium oxide-alcohol mixture was refluxed for three hours at 393 K, stirring continued for the entire reflux session.
3. The mixture was then allowed to cool to room temperature overnight.
4. Phosphorus acid of 85 % (H_3PO_4) was added in such a quantity to obtain the desired P/V atomic ratio.
5. The resulting solution was heated to 393 K and maintained under reflux with constant stirring for 2 hours.
6. The slurry was then centrifuged and filtered, washed and dried overnight in an oven at 423 K.

Calcination was then performed on the resulting precursor under a flow of *n*-butane/air mixture (0.75 % *n*-butane in air) at 673 K for 24 hours.

BET surface area of VPO catalyst produced via organic route ($18.4 \text{ m}^2/\text{g}$) was much higher than the VPO catalyst produced via aqueous route ($5.2 \text{ m}^2/\text{g}$). Besides, the catalyst prepared lower the desorption activation of oxygen which gave a higher mobility of lattice oxygen and bigger reduction site for oxidation of hydrocarbon. (Taufiq-Yap *et al.*, 2011)

2.2.3 Dihydrate Precursor Route

Vanadyl (IV) hydrogen phosphate dihydrate, $\text{VOPO}_4 \cdot 2\text{H}_2\text{O}$ was prepared as followed: (Hutchings *et al.*, 1994)

1. 5 g of V_2O_5 and 30 ml of phosphorus acid of 85 % (H_3PO_4) were refluxed in water (120 ml) for 24 hours.
2. The resulting precipitate was separated by filtration, washed with acetone and dried under ambient atmosphere.

The precipitate was identified as Vanadyl (IV) hydrogen phosphate dihydrate, $\text{VOPO}_4 \cdot 2\text{H}_2\text{O}$ using X-Ray Diffractometer (XRD) and Infrared Spectrometer (IR). Scanning Electron Microscopy (SEM) showed that the obtained $\text{VOPO}_4 \cdot 2\text{H}_2\text{O}$ consisted of platelet crystallites with lengths of approximately $20 \text{ }\mu\text{m}$. The surface area was about $1 \text{ m}^2/\text{g}$ after the evacuation at 423 K (Nakato *et al.*, 2000). On the other hand, $\text{VOPO}_4 \cdot 2\text{H}_2\text{O}$ also serve as the host which allow the intercalation of cation into the VPO catalyst. The cation acts as promoter to improve the catalytic performance of the catalyst. (Hutchings *et al.*, 1994)

2.2.4 Hemihydrate Precursor Route

Vanadyl (IV) hydrogen phosphate hemihydrate, $\text{VOHPO}_4 \cdot 0.5\text{H}_2\text{O}$, is one of the accepted precursors of the commercial VPO catalysts for selective oxidation of *n*-butane to MA. $\text{VOHPO}_4 \cdot 0.5\text{H}_2\text{O}$ was prepared as followed: (O'Mahony *et al.*, 2005)

1. V_2O_5 in a 90:10 mixture of 2-methyl propan-1-ol and benzyl alcohol were refluxed for 4 hours at $108 \text{ }^\circ\text{C}$.
2. 85 % of ortho-phosphorus acid solution was then added to the resulting vanadium suspension and was refluxed for a further 2 hours.

3. The reactant P/V mole ratio was 1:1.
4. Samples were recovered 120 min after phosphorus ($\text{o-H}_3\text{PO}_4$) addition. The recovered solids were filtered and dried at 120 °C.

$\text{VOHPO}_4 \cdot 0.5\text{H}_2\text{O}$ can be prepared via both aqueous and organic medium. However, the precursor obtained by the aqueous route is more crystalline. Whereas the organic route which utilized organic medium such as isobutanol as the reducing agent, results in platelet crystalline morphology producing rosette morphology due to the agglomeration of those platelets. (O'Mahony *et al.*, 2003)

2.2.5 Sesquihydrate Precursor Route

The focus of this research is based on sesquihydrate precursor route ($\text{VOHPO}_4 \cdot 1.5\text{H}_2\text{O}$). The sesquihydrate precursor was obtained by reducing $\text{VOPO}_4 \cdot 2\text{H}_2\text{O}$ in 1-butanol and calcined at temperature of 753 K over 10 hours in a flow of *n*-butane/ air mixture (0.75 % *n*-butane in air). (Ishimura *et al.*, 2000)

The synthesis of sesquihydrate precursor has been divided into a two-step procedure where $\text{VOPO}_4 \cdot 2\text{H}_2\text{O}$ served as the intermediate stage before reaching the precursor. (Ishimura *et al.*, 2000)

First step:

1. Vanadyl phosphate dihydrate, $\text{VOPO}_4 \cdot 2\text{H}_2\text{O}$ was prepared by reacting V_2O_5 (12.0 g from Fischer) with aqueous *o*- H_3PO_4 (115.5 g, 85 % from Fischer) in distilled water ($24 \text{ ml} \cdot \text{g}^{-1}$ solid).
2. The mixture was then stirred under reflux at 393 K for 24 h.
3. The brownish solid solution (colour of V_2O_5) has gradually changed to yellow.
4. The resultant yellow solid ($\text{VOPO}_4 \cdot 2\text{H}_2\text{O}$ phase) was then recovered by using centrifuge technique and subsequently washed sparingly with distilled water and oven dried at 353 K for 16 hours.

Second step:

1. 10.0 g of $\text{VOPO}_4 \cdot 2\text{H}_2\text{O}$ (50.5 mmol) was added to 150 ml of 1-butanol (PC Laboratory Reagent) and refluxed at 353 K for 24 h.
2. After being cooled to room temperature, the resultant precipitates which is whitish-blue powder ($\text{VOHPO}_4 \cdot 1.5\text{H}_2\text{O}$) was centrifuged out from the solvent, washed sparingly with acetone, and dried overnight (24h) in an oven at 353 K.

The sesquihydrate precursor obtained was calcined at 673 K in a reaction flow of 0.75 % *n*-butane/ air mixture. The catalysts that obtained could be used for instrumental analysis and catalytic test. (Ishimura *et al.*, 2000)

Employing 1-butanol as the reducing agent, the sesquihydrate precursor was obtained and activated at 673 K over 10 hours on-stream had revealed high specific activity in vapour-phase oxidation of *n*-butane. Besides, the sesquihydrate could be intercalated with cobaltous acetate to afford modified $(\text{VO})_2\text{P}_2\text{O}_7$ with high activity, but both selectivity to MA and surface area decreased with increasing cobalt contents. (Taufiq-Yap *et al.*, 2004)

The formation of a new phase (V^{5+}) and a decreased of the surface area of the catalysts were observed by extending the calcination duration of vanadyl pyrophosphate catalysts prepared via sesquihydrate precursor in *n*-butane/ air mixture at 673 K. The morphology of all the catalysts is shown to be in rosette-shape. However, significant changes were observed where the surface of the crystal platelet was getting cracked and rougher as the calcination duration increased. (Taufiq-Yap *et al.*, 2004)

2.3 Parameters of Vanadium Phosphorus Oxide Catalyst

The properties of Vanadium phosphorus oxide catalyst could be affected by several parameters, notably calcination conditions, support system, dopant used and finally the P/V atomic ratio. These factors could contribute to the formation of vanadyl

pyrophosphate and thus affect its selectivity and reactivity. However, the parameter concerned in this technical report is on the calcination duration.

2.3.1 Parameter: Calcination Condition

VPO catalyst is used in the selective oxidation of *n*-butane to MA. The most active phase that is used in the reaction is $(VO)_2P_2O_7$ which is well-crystallized. This catalyst possesses unique structural features to allow the activation of saturated hydrocarbon. $(VO)_2P_2O_7$ could be generated through calcinations of the precursor $VOHPO_4 \cdot 0.5H_2O$ prepared via reduction of $VOPO_4 \cdot 2H_2O$ using isobutanol as the reducing agent followed by thermal treatment in a reaction environment. (Bartholomew and Farrauto, 2006)

Calcination refers to a thermal treatment process in which the sample is being heated up to high temperature in oxygen or air with a specified environment. In other word, it is to heat up the precursor in order to activate the catalyst. As can be seen from the description of the process, transformation of precursor to the active phase could be affected by three main conditions of the calcinations which are temperature, environment and duration. (Bartholomew and Farrauto, 2006)

The temperature of the calcination could be adjusted in such a way that the intervals between all the experiments are the same for the ease of investigation. For instance, calcination was carried out at 200 °C, 400 °C, 600 °C and so on. As for calcination environment, flow of different chemical gas is introduced through the sample. Gases that can be used in this research are *n*-butane, propane and etc. Lastly, the durations for calcination can be manipulated by setting the intervals of all the experiments to be the same. For example, calcination is conducted for 24 hours, 48 hours, 72 hours and so on. Finally, samples generated under different conditions are compared with the physico-chemical tests. (Bartholomew and Farrauto, 2006)

2.3.2 Parameter: Support System

Supported VPO catalysts are more favourable than the unsupported ones as they offer several potential features such as better heat transfer character, larger surface

area to volume ratio of active component, better mechanical strength, and controllable catalyst textures. The VPO catalysts are usually supported by SiO_2 , TiO_2 , Al_2O_3 and SiC . It is noticed that, the existence of a support can result in support-oxide interaction that may hinder the formation of $(\text{VO})_2\text{P}_2\text{O}_7$ phase or bring about changes in phase composition. It has been reported that V^{5+} containing phase, such as $\alpha_1\text{-VOPO}_4$ or $\gamma\text{-VOPO}_4$, exists in supported VPO catalysts, especially in those prepared in aqueous media, and that the presence of such phases may lower *n*-butane conversion and/ or MA selectivity. (Ruiteenbeek* *et al.*, 1998)

2.3.3 Parameter: Dopant

The addition of dopant to VPO catalyst could enhance its activity and selectivity. A variety of cations could be incorporated into the crystal lattice of VPO. The presence of dopant could improve the surface phosphorus enrichment, which modified the surface acidity. Zazhigalov *et al.* (2003) proposed that the addition of cobalt could stabilize the catalyst performance by forming cobalt phosphate, which improves its catalytic properties. The cobalt addition acts as a structural promoter. The smallest amount of dopant produces the most beneficial effect. Moreover, they used in situ laser Raman spectroscopy to study the evolution of the catalyst structure for materials derived from $\text{Co-VOHPO}_4 \cdot 0.5\text{H}_2\text{O}$ formed by the reaction with isobutanol. They found that the incorporation of Co can modify the $\text{V}^{4+}/\text{V}^{5+}$ balance during the activation period and can therefore change the catalytic performance in the steady state. On the other hand, L. Cornaglia *et al.* (2003) used NMR techniques and it was observed that the presence of the Co dopant inhibits the transformation of the precursor and stabilizes on amorphous vanadium phosphate. (Kamiya *et al.*, 2003)

2.4 Maleic Anhydride

Maleic anhydride (MA), being an important commercial compound in chemical industry, is produced through the selective oxidation of *n*-butane in the presence of vanadyl pyrophosphate (VPO) as the catalyst. In 1995, the global production of MA was estimated at approximately 1.8 billion pounds, with an estimated value of \$700

million. Over the years, the world consumption has increased at an average annual rate of 5.8%, with the fastest growth occurring in Asia. The demand of MA comes primarily from the manufacture of unsaturated polyester resins, agricultural chemicals, food additives, lubricating oil additives and pharmaceutical. Hence, it is crucial that the productivity of MA could be enhanced and improved in order to meet the demanding market. (Xue, Zhi-yang, 1999)

2.4.1 Uses of Maleic Anhydride

Maleic anhydride, being a single molecule which possesses two distinctive types of chemical functions, has made itself more favourable in chemical industries. This feature has made it an extremely versatile potential chemical source of synthesis and industrial applications. In general, it is commonly used in the production of unsaturated polyester resins, lube oil additives, alkyd resins, and etc. The demand of this source increased gradually from 1995 where the average annual rate of world consumption rose up to 5.8% with the fastest growth occurring in Asia. (Felthouse *et al.*, 2001)

The primary usage of MA is in the production of polyester and alkyd resins. In our daily applications, resistant materials are needed in cars, trucks and pipelines. Resistant materials that used must be relatively strong to withstand the stress exerted and typically light for the ease of transportation. In addition, it must be corrosion resistant material. Thus, in the process of manufacturing, resins are usually integrated into fiberglass reinforced plastics in order to meet the three fundamental requirements as mentioned above. (Felthouse *et al.*, 2001)

On the other hand, MA is also an important source of material employed in the production lacquers, lube-oil additives and agricultural products. In lube-oil industry, the addition of MA decreases the drying time required for oils and enhances the coating quality of lacquers. Moreover, derivatives derived from MA could extend the intervals of the oil change and thus improve the performance and efficiency of the automotive engines. (Felthouse *et al.*, 2001)

Others uses of MA such as production of agricultural products. MA is also used in the manufacturing of herbicides, pesticides and plant growth regulators. Besides, fumaric and maleic acid which are commonly added in paper sizing resins as well as food and beverage acidulants, are important MA derivatives. The distribution of MA uses in 2000 year is tabulated in Table 2.1. (Sundmacher, 2006)

Table 2.1: Uses of Maleic Anhydride in year 2000

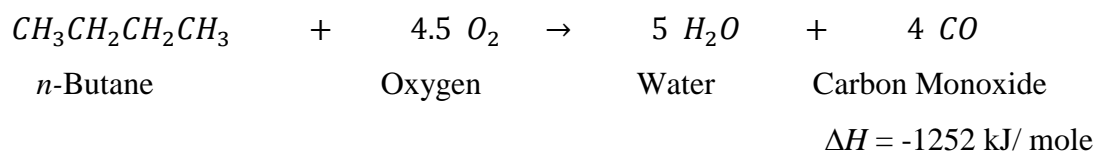
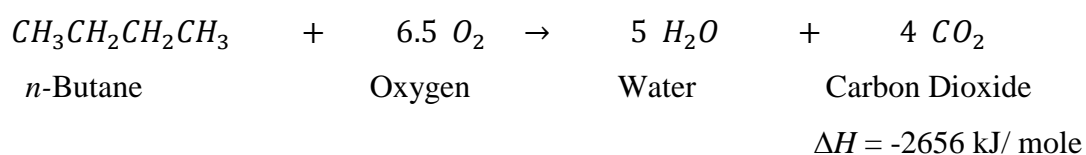
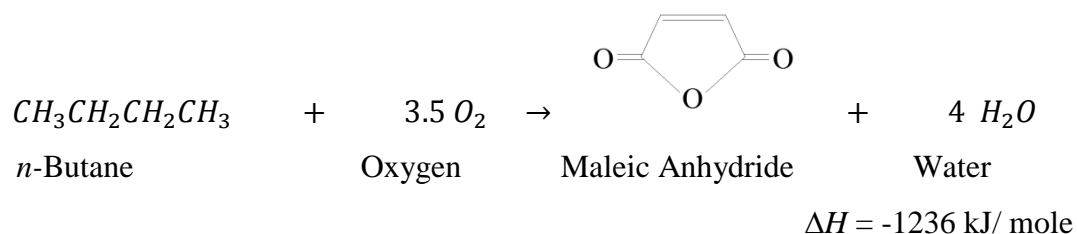
Market uses of MA	Distribution, %
Unsaturated polyester resins	63
Lubricating oil additives	10
Copolymers	9
Alkenyl succinic anhydrides	5
Maleic acid	3
Fumaric acid	2
Agricultural chemicals	1
Others	7

2.4.2 Oxidation of *n*-butane to Maleic Anhydride

Since 1980, approximately 225 patents in the United States have been issued on the MA technology. This results in a higher demand from market and thus the effort to understand and enhance the process is needed for optimum production. Catalyst, being the workhorse of almost the complete range of the chemical industry, is attracting a lot of attention from the researchers. Due to the complexity of this reaction, the catalyst used in this reaction has been getting a lot of attention. (Ruitenbeek *et al.*, 1998)

The transformation of MA from *n*-butane requires the abstraction of eight hydrogen atoms, three oxygen atoms inserted and a ring closure performed. This is a 14-electron oxidation that occurs exclusively on the surface of the solid catalyst. Moreover, this catalyst is the only commercial viable system that enables the selective production of MA from *n*-butane. (Felthouse *et al.*, 2001)

The partial oxidation of *n*-butane like benzene is very exothermic. As the following chemical equations show the energy released from *n*-butane oxidation exceeds that of benzene and this is reflected in the steam co-product. Below are the chemical reactions that show the energy released during the oxidation of *n*-butane: (Plotkin *et al.*, 2009)



The catalyst that plays the crucial role in this reaction is vanadium-phosphorus-oxide (VPO). As mentioned in section 2.2, it could be prepared by several methods. However, the most commonly seen and favourite method to prepare and generate VPO by the industry is the reaction of vanadium (V) oxide and phosphoric acid to form vanadyl hydrogen phosphate, $\text{VOHPO}_4 \cdot 0.5\text{H}_2\text{O}$. This precursor is then calcined in furnace to eliminate water from the structure and irreversibly form vanadyl pyrophosphate, $(\text{VO})_2\text{P}_2\text{O}_7$. Vanadyl pyrophosphate is the catalytically active phase required for the conversion of *n*-butane to MA. (Felthouse *et al.*, 2001)

CHAPTER 3

METHODOLOGY AND CHARACTERISATION TECHNIQUES

3.1 Materials and Gases used

Below are the chemicals used throughout this study:

1. Vanadium (V) pentoxide, V_2O_5 (Merck)
2. *ortho*-Phosphorus acid, $o\text{-H}_3\text{PO}_4$ (85%) (Merck)
3. 1-Butanol, $\text{CH}_3(\text{CH}_2)_3\text{OH}$ (R&M Chemicals)
4. Nitric acid, HNO_3 (R&M Chemicals)
5. Sulphuric acid, H_2SO_4 (95- 98%) (Merck)
6. Potassium permanganate, KMnO_4 (Fisher Scientific)
7. Ammonium iron (II) sulphate, $(\text{NH}_4)_2\text{Fe}(\text{SO}_4)_2$ (R&M Chemicals)
8. Diphenylamine, Ph_2NH (ACROS)
9. Ammonium Dihydrogen Phosphate, $\text{NH}_4\text{H}_2\text{PO}_4$ (Merck)
10. Ammonium metavanadate, NH_4VO_3 (Merck)

The gases used throughout this study:

1. 0.75 % *n*-butane in air (Malaysia Oxygen Berhad, MOX)
2. 99.99 % Purified Nitrogen (Malaysia Oxygen Berhad, MOX)
3. 99.99 % Purified Helium (Malaysia Oxygen Berhad, MOX)
4. 99.99 % Purified Argon (Malaysia Oxygen Berhad, MOX)
5. Liquefied Nitrogen Gas (Malaysia Oxygen Berhad, MOX)
6. Compressed Air (Malaysia Oxygen Berhad, MOX)

3.2 Methodology

Generally, the preparation of the bulk vanadyl pyrophosphate catalysts can take place via different routes; notably the sesquihydrate route (VPOs), the organic route (VPOo) and the reduction of Vanadyl phosphate dihydrate, $\text{VOPO}_4 \cdot 2\text{H}_2\text{O}$ phase (VPOd). The preparation of the doped vanadyl pyrophosphate catalysts can take place via organic route and the reduction of $\text{VOPO}_4 \cdot 2\text{H}_2\text{O}$ phase. In this research, the preparation of the vanadium phosphorus oxide catalyst takes place via the sesquihydrate precursor $\text{VOHPO}_4 \cdot 1.5\text{H}_2\text{O}$.

3.2.1 Preparation of the Vanadyl Phosphate Dihydrate

The production of vanadyl pyrophosphate catalyst has been developed via vanadyl hydrogen phosphate sesquihydrate precursor, $\text{VOHPO}_4 \cdot 1.5\text{H}_2\text{O}$. The synthesis of sesquihydrate precursor has been divided into two-step procedure, which involving vanadyl phosphate dihydrate, $\text{VOPO}_4 \cdot 2\text{H}_2\text{O}$ as an intermediate before obtaining the precursor. (Matsuura, 1995)

Firstly, 15 g of vanadium pentoxide, (V_2O_5) was weighed. It was then added with 90 ml of *ortho*-phosphorus acid, *o*- H_3PO_4 (85 %) and 360 ml of distilled water. The mixture was then refluxed for 24 hours at 120 °C. A yellow intermediate will be formed. The mixture was cooled to room temperature and was centrifuged. Yellow solids recovered by centrifuge technique, were washed sparingly with acetone and were oven-dried (~80 °C) for 24 hours. The yellow solids obtained are vanadyl phosphate dehydrate ($\text{VOPO}_4 \cdot 2\text{H}_2\text{O}$). (Hutchings *et al.*, 1994)

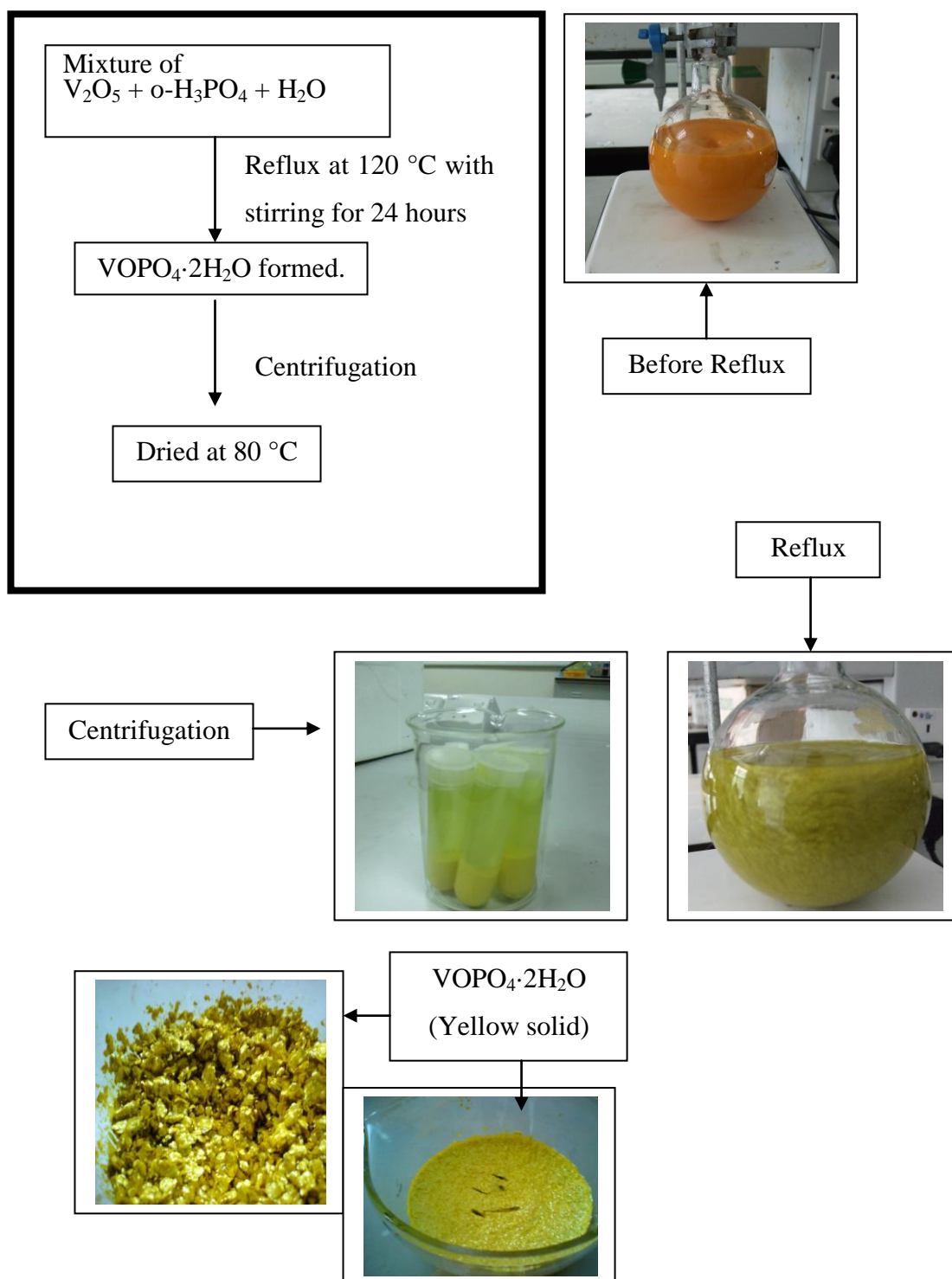


Figure 3.1: Diagrams show the preparation steps of the $\text{VOPO}_4 \cdot 2\text{H}_2\text{O}$

3.2.2 Preparation of Vanadium Phosphorus Oxide Catalysts

10 g of $\text{VOPO}_4 \cdot 2\text{H}_2\text{O}$ precursors were added with 150 ml 1-butanol. The mixture was then under reflux for 24 hour. After being cooled to room temperature, the resultant precipitate which is whitish-blue powder is referred to vanadyl hydrogen phosphate sesquihydrate precursor. Whitish-blue powder was recovered by centrifuge technique and oven-dried at 80 °C for 24 hours. (Hutchings *et al.*, 1994)

The resulting powder was then undergone calcinations in a reaction flow of 0.75 % *n*-butane in air mixture of the 400 °C for each of the following duration: 24, 48, 72 and 96 hours.

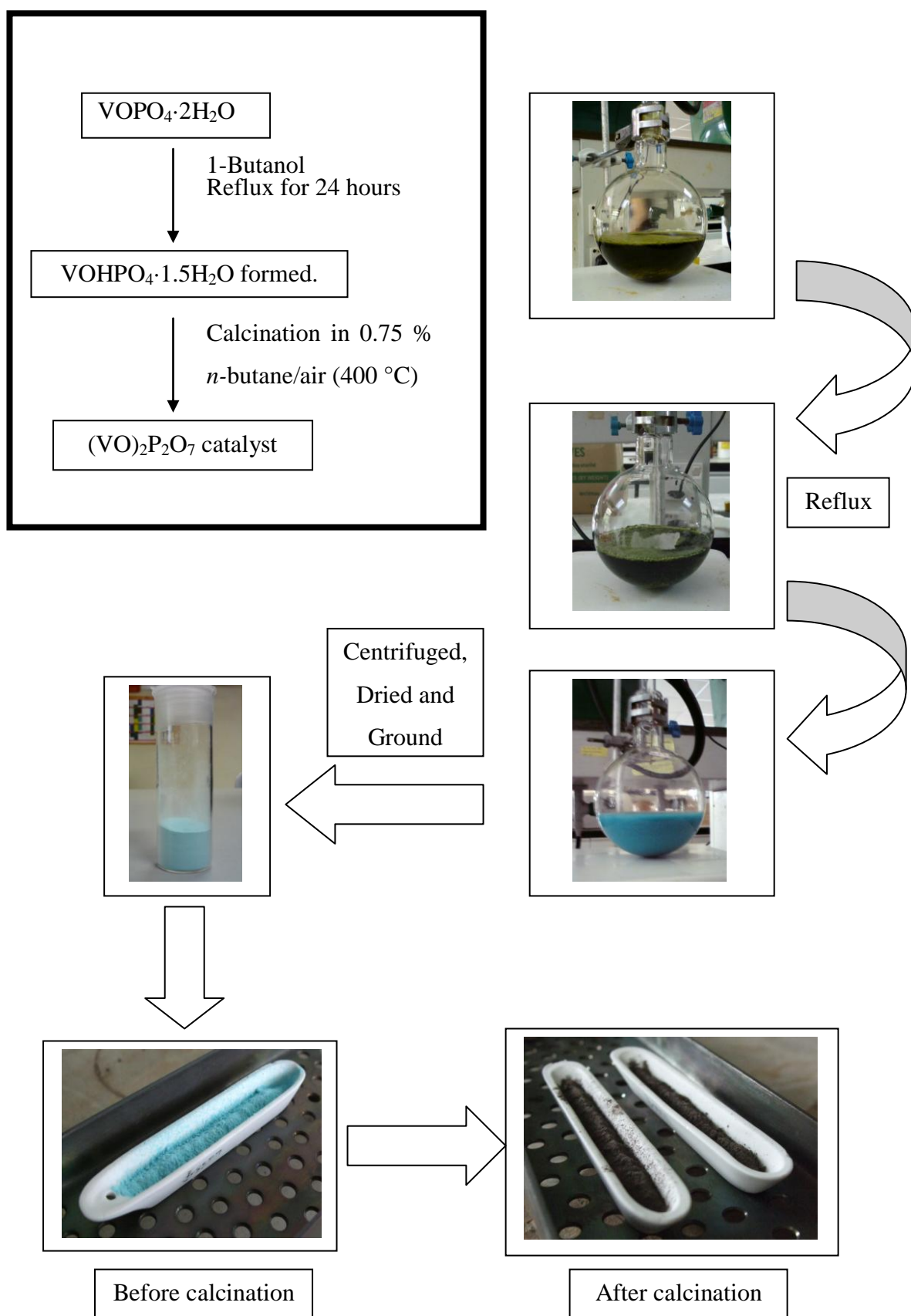


Figure 3.2: Diagrams show the preparation steps of the $(VO)_2P_2O_7$

3.3 Characterisation Techniques and Instrumentations

Throughout the research, there are some instruments involved to examine the physical and chemical properties of the catalysts produced. They are used to analyse the catalyst formed, which is vanadyl pyrophosphate catalyst. The machines and techniques used are notably, X-Ray Diffractometer, BET surface area measurement, Scanning Electron Microscopy with Energy Dispersive X-Ray Spectrometer (SEM-EDX), Redox Titration and Inductively-Coupled Plasma- Optical Emission Spectrometer (ICP- OES).

3.3.1 X-Ray Diffraction (XRD) Analysis

X-Ray Diffraction (XRD) Analysis is a machine used to determine the phase composition of catalyst at ambient temperature and under normal atmospheric conditions. It is one of the most powerful and efficient techniques for qualitative and quantitative analysis of crystalline compounds. It relies on the dual wave or particle nature of X-Rays to obtain information about the structure of crystalline materials. The sample is prepared for analysis by packing a small amount of sample into a shallow cup. Sometimes the sample can be introduced as slurry and placed on a quartz slide. (Masilo, 2009)

The phenomenon of diffraction occurs when the penetrating radiation, X-rays enters a crystalline substance and is scattered. The scattered X-Rays will undergo constructive and destructive interference in a process termed as diffraction. In order for a beam to be 100 % diffracted, the distance it travels between rows of atoms at the angle of incidence must be equal to an integral multiple of the wavelength of the incident beam. D-spacings which are greater or lesser than the wavelength of the directed X-ray beam at the angle of incidence will produce a diffracted beam of less than 100 % intensity. Sample will rotate during the analysis to reduce any heating to the sample. Resulting diffractogram will confirm the identity of a solid material as a pharmaceutical powder. The diffraction of X-Rays by crystals is described by Bragg's Law. X-Rays are reflected from a crystal only if the angle of incidence satisfies the condition $n\lambda = 2d \sin \theta$. (Chorkendorff and Niemantsverdriet, 2003)

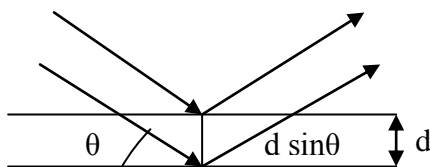


Figure 3.3: X-rays scattered by atom in an ordered lattice interfere

X-ray diffraction has been in use in two main areas; the fingerprint characterization of crystalline materials and the determination of their structure. Each crystalline solid has its unique characterization X-ray powder pattern which may be used as a “fingerprint” for its identification. Once the material has been identified, X-ray crystallographic may be used to determine its structure, *i.e.* how the atoms pack together in the crystalline state and what the interact-atomic distance and angle are *etc.* therefore, size and the shape of the unit cell for any compound most easily determined by using the diffraction of X-rays. In catalysis, X-ray diffraction analysis is carried out to determine the phase compositions of catalysts at ambient temperature and under normal atmospheric conditions. Therefore, the relative abundance of V^{4+} and V^{5+} can be determined. The crystallite sizes can also be determined by using Debye-Scherrer equation: (Chorkendorff and Niemantsverdriet, 2003)

$$t = \frac{0.89\lambda}{\beta_{hkl} \cos \theta_{hkl}}$$

Where t is the crystallite size for $(h\ k\ l)$ phase, λ is the X-ray wavelength of radiation for $CuK\alpha$, β_{hkl} is the full-width at half maximum (FWHM) at $(h\ k\ l)$ phase and θ_{hkl} is the diffraction angle for $(h\ k\ l)$ phase. (Klug and Alexander, 1974)

In this study, X-ray diffraction (XRD) patterns were obtained using a Shimadzu diffractometer model XRD-6000 employing $CuK\alpha$ radiation generated by a Philips glass diffraction X-ray tube broad focus 2.7 kW type on the catalysts at ambient temperature. The basal spacing was determined via powder technique. The samples were scanned at the range $2\theta = 2^\circ - 60^\circ$ with a scanning rate of $1.2000^\circ \text{ min}^{-1}$. The diffractograms obtained were matched against the Joint Committee on Powder Diffraction Standards (JCPDS) PDF1 database version 2.6 to confirm the catalysts phases. (Klug and Alexander, 1974)



Figure 3.4: Shimadzu diffractometer model XRD-6000

3.3.2 BET Surface Area Measurements

The Brunauer-Emmett-Teller (BET) surface area analysis involves the nitrogen adsorption at low temperature has been used for the determination of the single point surface area of porous materials, using Thermo Finnigan Sorptometric 1990. BET analysis is an important method which provides information regarding the porous nature and the surface area of the materials prepared by applying physical adsorption of gas molecules on the solid surface. (Jacobson and Mellon, 2002)

The catalysts in powder form were heated and degassed in a flow of purified nitrogen gas. This is to eliminate any unwanted adsorbed molecules prior to analysis. During the analysis, the sample was placed inside a vacuum chamber at a constant temperature of liquid nitrogen. The sample was then subjected to a wide range of pressures in order to generate adsorption or desorption isotherms. (Masilo, 2009)

In fact, BET analysis's principle is an extension, or rather a continuation from Langmuir theory, which is a theory for monolayer molecular adsorption, to multilayer adsorption with the following hypotheses: (Jacobson and Mellon, 2002)

- i. Gas molecules physically adsorb on a solid in layers infinitely;
- ii. There is no interaction between each adsorption layer; and

- iii. The Langmuir theory can be applied to each layer.

BET can be represented by the following equation: (Masilo, 2009)

$$\frac{1}{v[(P_o/P) - 1]} = \left(\frac{c-1}{v_m c}\right) \left(\frac{P}{P_o}\right) + \frac{1}{v_m c}$$

Where

P = equilibrium pressure of adsorbates at the adsorption temperature

P_o = saturation pressure of adsorbates at the adsorption temperature

v = adsorbed gas quantity (unit: volume)

v_m = monolayer adsorbed gas quantity

c = BET constant

$= \exp\left(\frac{E_1 - E_L}{RT}\right)$ where E_1 is the heat of adsorption for the first layer;

E_L is the heat of adsorption for second and higher layers
and it is equal to the heat of liquefaction.



Figure 3.5: Thermo Finnigan Sorptometric 1990

3.3.3 Redox Titration

This method was developed by Miki Niwa and Yuichi Murakami in 1982. They had investigated the reaction mechanism of the ammoxidation of toluene on V_2O_5/Al_2O_3 catalyst. The bifunctional activity of this catalyst which consists of the oxidation activity of V_2O_5 and the dehydration property of Al_2O_3 is stressed. However, some problems about the active sites of vanadium oxide and alumina and how they actually contribute to the ammoxidation of toluene remain a question. (Niwa and Mukakami, 1982)

In this research, redox titration was carried out to determine the average vanadium valance (AV) of the VPO catalysts and/ or to obtain the average oxidation state of vanadium. First, a known amount of the sample is dissolved in 100 ml sulphuric acid (2 M). It is then cooled to room temperature before being titrated with potassium permanganate solution (0.01 N). This titrant is used to oxidize V^{3+} and V^{4+} in the solution to V^{5+} . The end point is reached when the change of colour from the original greenish blue to pink was observed. The volume of potassium permanganate used was recorded as V_1 . Then the oxidized solution was treated with ammonium iron (II) sulphate solution (0.01 N). This is to reduce V^{5+} to V^{4+} in the solution. Diphenylamine is used as an indicator. The end point is reached when the purple colour of the solution disappeared and became colourless. The volume of ammonium iron (II) sulphate used was recorded as V_2 . (Niwa and Mukakami, 1982)

Another fresh 25 ml of the original solution was then titrated with 0.01 N ammonium iron (II) sulphate solution. Diphenylamine is also used as indicator. This stage of titration is to determine the V^{5+} in the original solution. The end point is reached when the solution changes from purple to greenish blue. The volume of ammonium iron (II) sulphate solution used was recorded as V_3 . (Niwa and Mukakami, 1982)

The average oxidation state of vanadium (AV) can be determined by solving the equation below: (Niwa and Mukakami, 1982)

$$AV = \frac{5V^{5+} + 4V^{4+} + 3V^{3+}}{(V^{5+} + V^{4+} + V^{3+})}$$

where V^{3+} , V^{4+} and V^{5+} are concentration of vanadium at different oxidation state. In order to obtain values for V^{3+} , V^{4+} and V^{5+} values, respectively. The following equations are used:

$$V^{3+} = 20(0.01)V_1 - 20(0.01)V_2 + 20(0.01)V_3$$

$$V^{4+} = 40(0.01)V_2 - 40(0.01)V_3 - 20(0.01)V_1$$

$$V^{5+} = 20(0.01)V_3$$

where V_1 = the volume of potassium permanganate used and V_2 = the volume of ammonium iron (II) sulphate used. (Niwa and Mukakami, 1982)



Figure 3.6: Diagram shows the experiment of Redox Titration

3.3.4 Scanning Electron Microscopy with Energy Dispersive X-ray Spectrometer (SEM-EDX)

SEM provides high magnification imaging of almost all materials whereas EDX measures X-rays that are emitted during electron bombardment in an electron microscope (SEM or TEM) to determine the chemical composition of materials based on the micro- and nano- scale. (Kotula *et al.*, 2006)

Combining both the spectroscopes make possible to find out which element different parts of a sample comprises. The instrument is very suitable for different kinds of investigations. The SEM-EDX technique could identify the critical characteristics of particles. It offers the ability to gather information about finer

particles than by optical microscopes and can readily distinguish between clusters and agglomerates of particles in addition to chemical analysis available by EDX. The strength of this analysis technique is its ability to gather statistically significant data on the size, morphology and composition of the particles in a time efficient manner, beyond the capabilities of conventional optical microscopy. (Kotula *et al.*, 2006)

Scanning electron microscope incorporated with energy dispersive X-ray analytical system, Hitachi S-3400 N could determine the catalyst's structure, as well as the elemental composition. These analyses require only a small amount of catalyst sample. For EDX characterization, the atoms of the surface of the catalyst powders are excited by the electron beam from the SEM, emitting specific wavelengths which are characteristic of the atomic structure of the elements. (Masilo, 2009)

Firstly, a thin layer of gold metal is required to be coated on the surface of the catalyst sample for conductive purposes during the analysis. The analysis begins by focusing a finely collimated beam of electrons into a small probe, which scans across the surface of the specimen. The interaction between the beam and the sample result in the emission of the electrons and photons, as the electrons penetrates the surface of the sample. Following this, the emitted particles are then collected and sent to the detector to provide information regarding the surface morphology. (Masilo, 2009)



Figure 3.7: Hitachi S-3400N

3.3.5 Inductively-Coupled Plasma- Optical Emission Spectroscopy (ICP-OES)

ICP-OES is a sophisticated instrument used to detect the trace elements. Quantitative and qualitative analysis of the VPO catalysts were performed on a Perkin- Elmer Emission Spectrometer Model Plasma 1000. The molar ratios of the elements, P/V ratios were determined using this technique. The catalyst samples were digested in 10 mL of 8 M nitric acid (HNO_3) to release the metal elements into solution for analysis. (Masilo, 2009)

The multi elemental standards of the elements under research were prepared in the 6.25 to 50 ppm concentration range for vanadium and phosphorus. The actual concentrations of the existing elements in the samples were determined from this range of standards using the calibration graphs obtained from the element standards. The range of elemental standards used for the analysis is given in Table 3.1. (Masilo, 2009)

Table 3.1: The range of calibration standards used in the ICP- OES

Element	Concentration Range (ppm)			
Vanadium, V	50.00	25.00	12.50	6.25
Phosphorus, P	50.00	25.00	12.50	6.25

In this technique, the sample is aspirated into an inductively coupled plasma discharge. The analyte is then converted into the gas-phase atoms in their excited states. Following this, the emitted light produced by the excited atoms is measured relative to the concentration range of the standards to give the sample concentration. (Masilo, 2009)

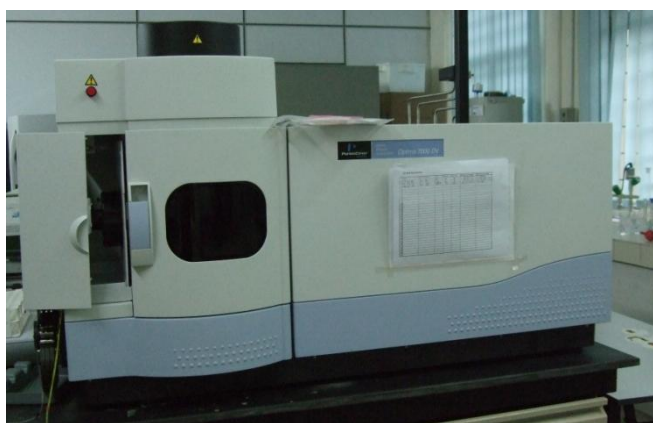


Figure 3.8: Perkin- Elmer Emission Spectrometer Model Plasma 1000

CHAPTER 4

RESULTS AND DISCUSSION

4.1 Introduction

The physical and chemical performances of the Vanadyl Pyrophosphate Catalysts obtained via different calcination durations have been scrutinized under various instrumental analyses, namely:

- i. X-Ray Diffraction (XRD)
- ii. Brunauer-Emmer-Teller Single Point Surface Area (BET)
- iii. Scanning Electron Microscopy (SEM)
- iv. Redox Titration
- v. Energy Dispersive X-Ray Diffraction (EDX)
- vi. Inductively-Coupled Plasma- Optical Emission Spectrometer (ICP-OES)

In this chapter, catalysts obtained via calcination durations of 24, 48, 72 and 96 hours are denoted as VPO24, VPO48, VPO72 and VPO96, respectively.

4.2 X-Ray Diffraction (XRD)

The XRD patterns of the four catalysts obtained via different calcination durations of the same precursor at 733 K under the flow of *n*-butane (0.75% *n*-butane in air), *i.e.*, 24, 48, 72 and 96 hours, are presented in Figure 4.1. The intensities of the peaks show that these catalysts have a well crystallized $(VO)_2P_2O_7$ phase. The presence of $(VO)_2P_2O_7$ is recognized by the pyrophosphate peaks at $2\theta = 22.89^\circ$, 28.47° and 29.94° , which correspond to $[0\ 2\ 0]$, $[2\ 0\ 4]$ and $[2\ 2\ 1]$ planes, respectively. From the 2θ obtained, the particles' size for each plane was calculated from the 2θ obtained and tabulated in Table 4.1. Formula employed for this calculation is attached in Appendix C.

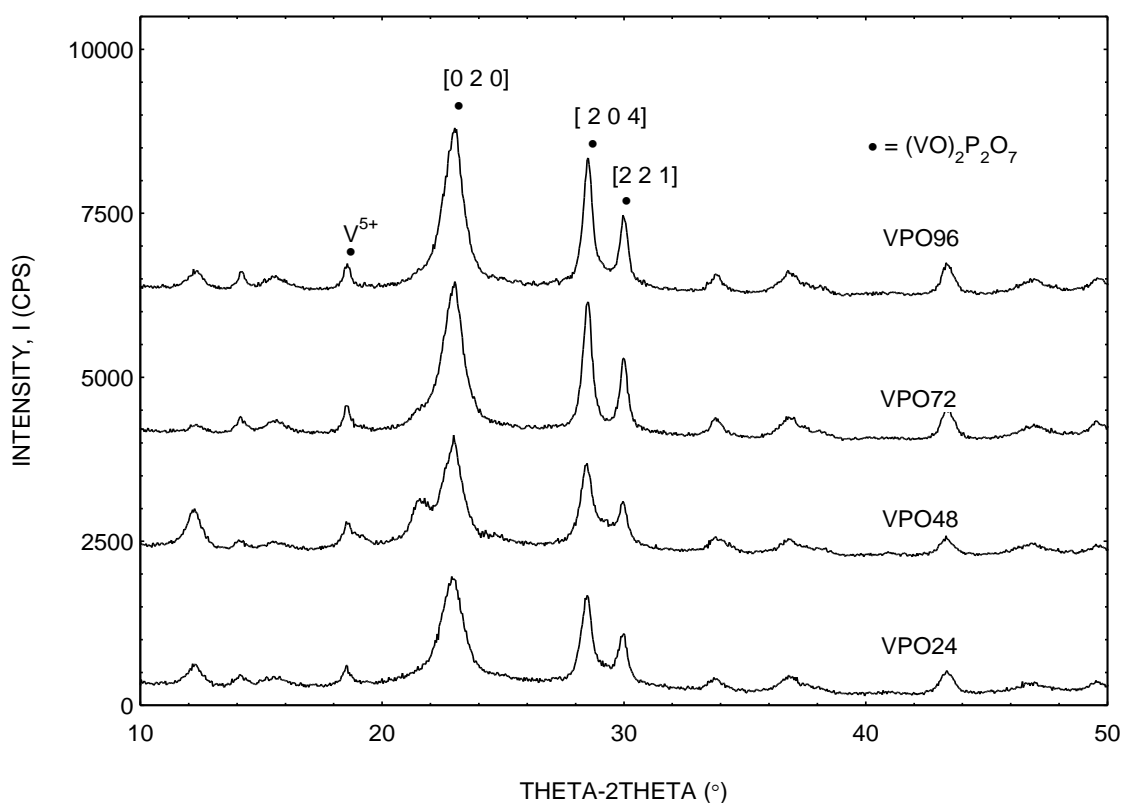


Figure 4.1: XRD Profiles for Different Calcination Duration

From Table 4.1, it can be concluded that, as the calcination duration increased, the particle size of plane $[0\ 2\ 0]$ increased as well. However, the relationship between $[2\ 0\ 4]$ and $[2\ 2\ 1]$ planes with calcination durations could not be developed.

Table 4.1: Particles' size of each plane for each sample

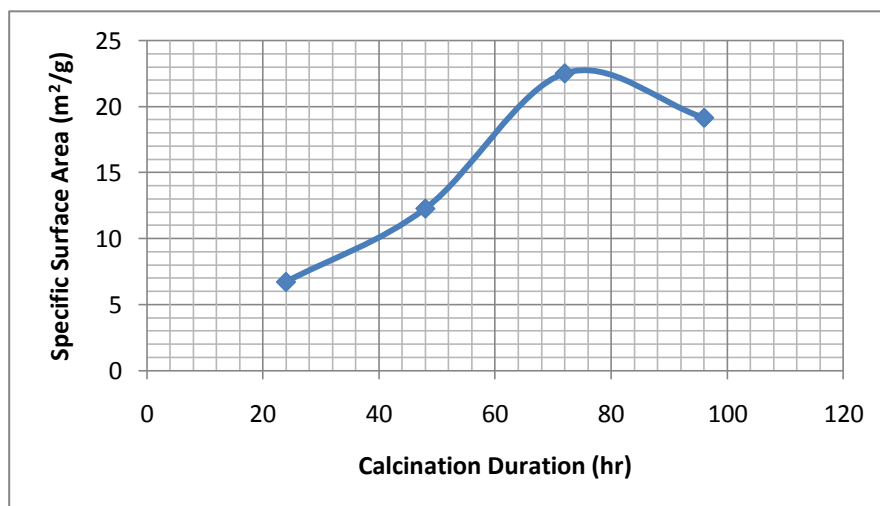
Sample	Particle Size, T (Å)		
	[0 2 0]	[2 0 4]	[2 2 1]
VPO24	74.171	128.339	127.829
VPO48	78.759	116.939	93.137
VPO72	83.375	144.252	152.330
VPO96	84.640	141.029	144.659

4.3 Brunauer-Emmer-Teller Single Point Surface Area (BET)

By extending the calcination duration, an increase of specific surface area of the VPO catalysts was observed. However, the surface area dropped for VPO96, concluding that calcination duration of 3 days is sufficient enough to provide the most specific surface area for reaction to occur. The decrease in specific surface area of VPO96 could probably caused by sintering effect. Sintering, also known as aging, refers to the loss of catalytic activity due to a loss of active surface area resulting from the prolonged exposure to high gas-phase temperature. The active surface area may be lost either by crystal agglomeration and surface recrystallization or the formation or elimination of surface defects. (Fogler, 2006)

Table 4.2: BET Surface Area for each sample

Sample	Specific Surface Area (m ² /g)
VPO24	6.733
VPO48	12.286
VPO72	22.525
VPO96	19.157



Graph 4.1: Correlation between Calcination Duration and Specific Surface Area

4.4 Scanning Electron Microscopy (SEM)

Scanning electron microscopy shows the surface morphologies of the catalysts obtained via different calcination durations. Nonetheless, the principal structures of the catalysts are still the same where they consist of plate-like crystals, which are arranged into the characteristics rosette-shape clusters. The catalysts which had been calcined for the 72 hours, VPO72, appeared to have clearer and more prominent rosette-shape agglomerates when compared to the less calcined and over-calcined sample. By increasing the calcination duration, a consistency whereby the amount of rosebud-shape agglomerates rises is observed. However, the plate-like crystals of VPO96 adhere closer to each other, resulting in crystal agglomeration which in turn causes a decrease in specific surface area. The rosette-type agglomerates are made up of $(VO)_2P_2O_7$ platelets that preferentially expose $[0\ 2\ 0]$ crystal planes. (Hutchings *et al.*, 1995)

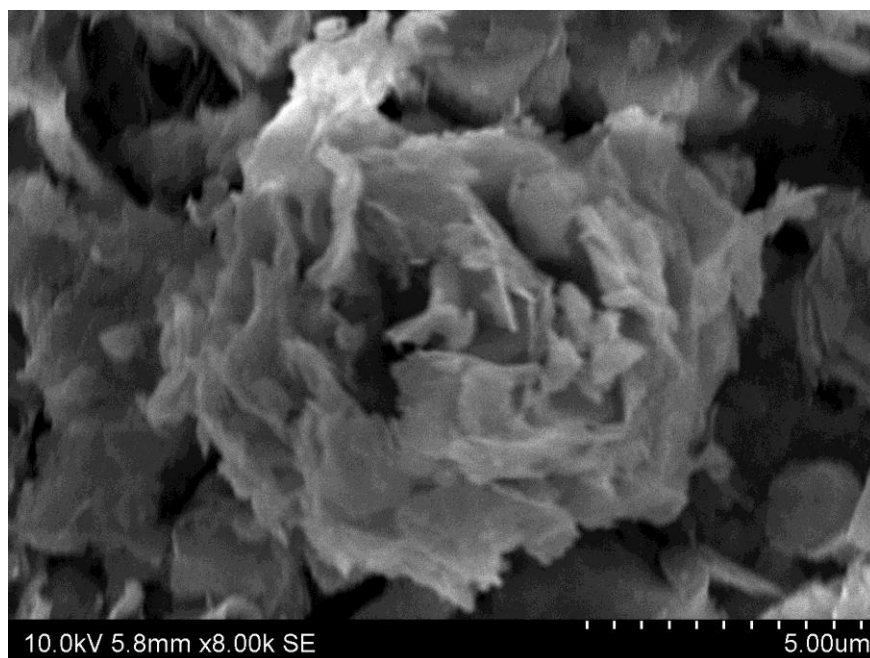


Figure 4.2: SEM Image of VPO24

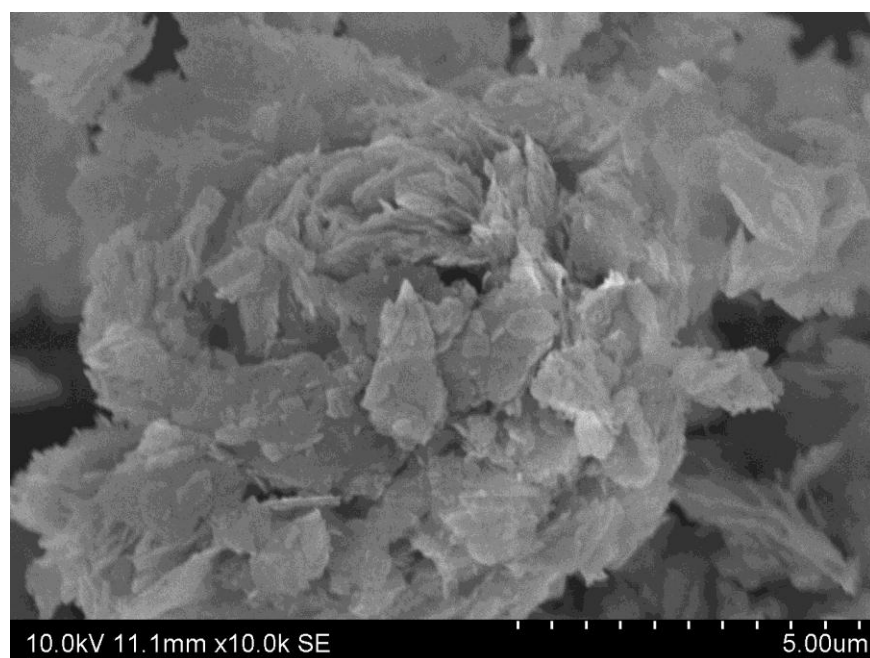


Figure 4.3: SEM Image of VPO48

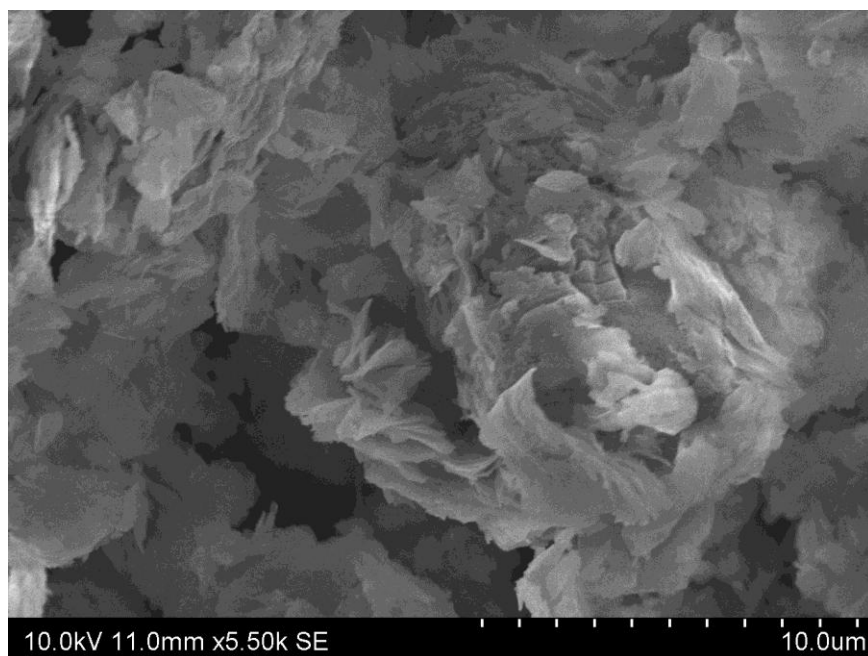


Figure 4.4: SEM Image of VPO72

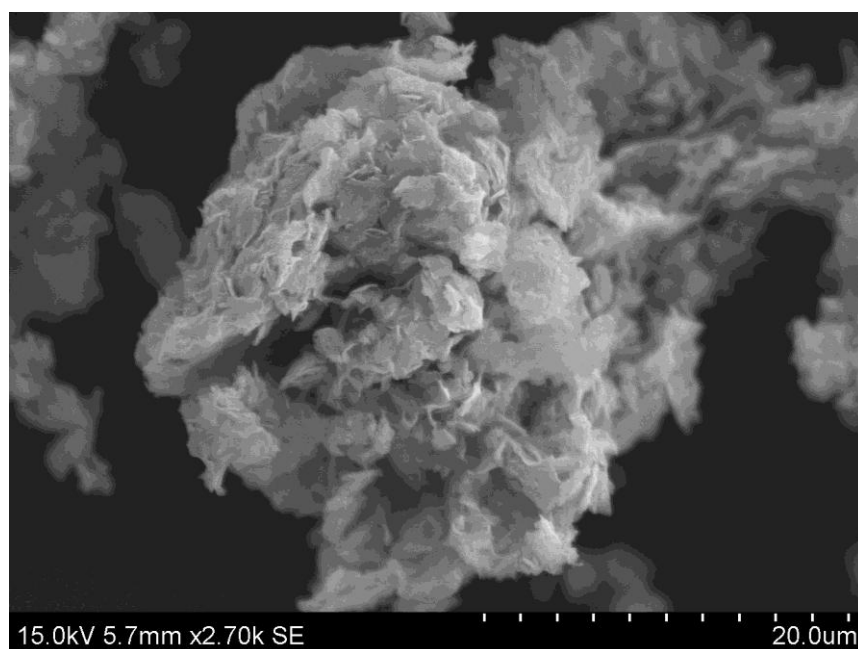


Figure 4.5: SEM Image of VPO96

4.5 Redox Titration

Redox titrations were carried out to determine the average oxidation state of vanadium in the sample. The average oxidation numbers of vanadium for different calcination durations are summarized in Table 4.3. From the data obtained in table, the average oxidation state lies closely to 4.00 for all the catalysts. Comparing to the XRD profiles in Figure 4.1, the amount of V^{5+} phase is in close agreement to the intensity of V^{5+} peak. The result reflects that oxidized phase of V^{5+} such as $VOPO_4$ exist in the catalysts. However, there is no specific trend of the amount of V^{5+} phase. Thus the correlation between the average oxidation number and calcination durations could not be established. VPO catalysts characterized with a high V^{5+} content have high selectivity but lower activity. (Gulians and Carreon, 2005)

Table 4.3: V_{AVERAGE} for each sample obtained

Sample	V_{AV}	V^{5+} (%)	V^{4+} (%)
VPO24	4.124	12.4	87.6
VPO48	4.277	27.7	72.3
VPO72	4.111	11.1	88.9
VPO96	4.113	11.3	88.7

4.6 Inductively- Coupled Plasma- Optical Emission Spectrometer (ICP-OES)

The P/V atomic ratio obtained for ICP-OES are summarized in Table 4.4. The P/V atomic ratios for all sample obtained show a slightly excessive of phosphorus in the samples. However, with the excessive phosphorus, it helps to stabilize the V^{5+} oxidation state. Moreover, it limits the over-oxidation of $(VO)_2P_2O_7$ to $VOPO_4$ in the reactant's atmosphere and air (Taufiq-Yap *et al.*, 2008). Cavani *et al.* (2005) have also reported that P/V ratio is one of the key factors in catalysts preparation to avoid the oxidation of $(VO)_2P_2O_7$ and/ or of the intermediate amorphous phase to a V^{5+} phosphate. However, it seems clear from the results obtained that the P/V atomic

ratios did not depend strongly upon the durations of calcination and/ or calcination atmosphere.

Table 4.4: P/V atomic ratio

Sample	Concentration of phosphorus, P (mg/L)	Concentration of vanadium, V (mg/L)	P/V Ratio
VPO24	20.00	28.38	1.16
VPO48	18.13	24.42	1.22
VPO72	21.96	32.89	1.10
VPO96	19.64	29.06	1.11

4.7 Energy Dispersive X-Ray Diffraction (EDX)

EDX was conducted to confirm the results obtained from ICP-OES. This technique provides information about the elemental ratio at the surface of the catalysts. From Table 4.5, it is observed that the P/V ratios obtained do not match with the results from ICP-OES, Table 4.4. The difference between the results is most likely caused by the technique of analysis. ICP-OES requires the catalysts to be in solution phase, which could ensure a more accurate measurement whereas EDX detects only on the surface of the catalysts. Furthermore, a lower P/V ratio observed in the EDX was also expected since EDX is a surface technique, penetrating only a few microns of the catalysts. However, VPO72 possessed a higher P/V ratio than ICP. (Masilo, 2009)

Table 4.5: P/V atomic ratio

Sample	Phosphorus, P (at%)	Vanadium, V (at%)	P/V Ratio
VPO24	25.23	27.86	0.91
VPO48	23.87	20.99	1.14
VPO72	18.77	16.02	1.17
VPO96	23.66	24.13	0.98

CHAPTER 5

CONCLUSION AND RECOMMENDATIONS

5.1 Conclusions

In conclusion, all catalysts possess good crystalline with characteristic peaks of vanadyl pyrophosphate phase in the XRD profiles and their surface morphologies were found to be close to rosette-shape. Besides, it was found that VPO catalyst obtained via 3 days calcination gives the highest specific surface area, which indicates it has the highest activity among all. From the redox titration, the results exhibit that oxidized phase such as V^{5+} exists in the catalysts. However, the correlation between the calcination durations and the average oxidation number of vanadium could not be established. The P/V ratios obtained via ICP-OES lie closely to ratio of 1.0. Again, from the data obtained it is concluded that the P/V ratio did not depend strongly upon the calcination durations. Finally, the P/V ratios obtained via EDX agree closely with the P/V ratios obtained via ICP-OES.

5.2 Recommendations

In this technical report, the physico-chemical properties of the VPO catalysts obtained via different calcination durations have been presented. However, the selectivity and activity of VPO catalysts were not tested. Hence, catalytic test should be conducted in order to scrutinize both its selectivity and activity.

REFERENCES

- Bartholomew and Farrauto. (2006)). Fundamentals of Industrial Catalytic Processes. (2nd ed.). Published by Wiley.
- B. Dmuchovsky and J. E. Franz. (1967). Maleic Anhydride. *Encyclopedia of Chemical Technology, Volume 12*. Published by Wiley.
- B. Viswanathan *et al.*. (2002). Catalysis Principles and Applications. Published by Narosa.
- C. H. Bamford *et al.*. (1993) Comprehensive Chemical Kinetics.
- H. Scott Fogler. (2008). Elements of Chemical Reaction Engineering (4th ed.) Published by Pearson, Prentice Hall.
- I. Chorkendorff and J.W. Niemantsverdriet. (2003). Concepts of Modern Catalysis and Kinetics. Published by Wiley.
- Israel E. Wachs. (1997). Fundamental Studies of Butane Oxidation over Model-Supported Vanadium Oxide Catalysts: Molecular Structure-Reactivity Relationships. Published in *Journal of Catalysis* 170, 75- 88.
- Jay B. Benziger *et al.*. (1997). New Precursors to Vanadium Phosphorus Oxide Catalysts. Published by Elsevier in *Catalysis Today* 33 (1997) 49- 56.
- Jeffery S. Plotkin and Alexander Coker. (2009). Maleic Anhydride (MAN). Published by Nexant.
- L. O'Mahony *et al.*. (2005). Phase Development and Morphology During the Thermal Treatment of $\text{VOHPO}_4 \cdot 0.5\text{H}_2\text{O}$. Published by Elsevier in *Applied Catalysis A: General* 285 (2005) 36- 42.
- Louisa Griesel *et al.*. (2004). Preparation of vanadium Phosphate Catalysts from $\text{VOPO}_4 \cdot 2\text{H}_2\text{O}$. Published by Elsevier in *Journal of Molecular Catalysis A: chemical* 220 (2004) 113- 119.

- M. Ruitenbeek* *et al.*. (1998). Effects of Silica and Titania Supports on the Catalytic Performance of Vanadium-Phosphorus-Oxide Catalysts. Published by Elsevier Science B. V..
- Michel Abon* and Jean-Claude Volta. (1997). Vanadium Phosphorus Oxides for *n*-butane Oxidation to Maleic Anhydride. Published by Elsevier in *Applied Catalysis A: General* 157 (1997) 173- 193.
- Neoentle Masilo. (2009). *n*-butane Activation over Ruthenium and Iron Promoted VPO Catalysts.
- Paul G. Kotula *et al.*. (2006). SEM/ EDX Spectrum Imaging and Statistical Analysis of A Metal/ Ceramic Braze.
- P. J. G. Butler *et al.*. (1969). The Use of Maleic Anhydride for the Reversible Blocking of Amino Groups in Polypeptide Chains. Published in *Biochemistry Journal* 112.
- Taufiq-Yap *et al.*. (2001). The Effect of the Duration of *n*-butane/ air Pretreatment on the Morphology and Reactivity of (VO)₂P₂O₇ Catalysts . Published in *Catalysis Letters* Vol. 74, No. 1-2, 2001.
- Taufiq-Yap *et al.*. (2001). Physico-Chemical Characterisation of Vanadium-Phosphorus-Oxide Catalysts Prepared in Organic and Aqueous Medium. Published by *Jurnal Teknologi*, 34 (C) Jun 2001: 17- 24.
- Taufiq-Yap *et al.*. (2004). Synthesis and Charaterisations of Vanadyl Pyrophosphate Catalysts via Vanadyl Hydrogen Phosphate Sesquihydrate Precursor. Published in *Catalysis Today* 93-95, 715- 722.
- Timothy R. Felthouse *et al.*. (2001). Maleic Anhydride, Maleic Acid and Fumaric Acid.
- Vadim v. Guliants and Moises A. Carreon. (2005). Vanadium-Phosphorus-Oxides: from Fundamentals of *n*-Butane Oxidation to Synthesis of New Phase.
- Xue, Zhi-yang. (1999). In-situ Vibrational Spectroscopic Investigation of C*H* Hydrocarbon Selective Oxidation over Vanadium-Phosphorus-Oxide Catalysts.
- Yuichi Kamiya *et al.*. (2003). Selective Oxidation of *n*-butane over Iron-doped Vanadyl Pyrophosphate Prepared from Lamellar Vanadyl *n*-hexylphosphate. Published by Elsevier in *Applied Catalysis A: General* 253 (2003) 1-13.

APPENDICES

APPENDIX A: Volume of Isobutanol Used

Molecular formula of vanadyl phosphate dihydrate = $\text{VOPO}_4 \cdot 2\text{H}_2\text{O}$

Molecular weight of Vanadium = 50.9414 g/mol

Molecular weight of Phosphate = 30.97376 g/mol

Molecular weight of Oxygen = 15.9994 g/mol

Molecular weight of Hydrogen = 1.0079 g/mol

$$\begin{aligned} \text{Molecular weight of } \text{VOPO}_4 \cdot 2\text{H}_2\text{O} &= 50.9414 \text{ g/mol} + (7 \times 15.9994 \text{ g/mol}) + \\ &\quad 30.97376 \text{ g/mol} + (4 \times 1.0079 \text{ g/mol}) \\ &= 197.94256 \text{ g/mol} \end{aligned}$$

$$\begin{aligned} \text{No. of mol of } \text{VOPO}_4 \cdot 2\text{H}_2\text{O} &= \frac{\text{mass}}{\text{molecular weight}} \\ &= \frac{10 \text{ g}}{197.94256 \text{ g/mol}} \\ &= 0.05052 \text{ mol} \end{aligned}$$

(50 mol alcohol/ mol $\text{VOPO}_4 \cdot 2\text{H}_2\text{O}$)

For 1 mol of $\text{VOPO}_4 \cdot 2\text{H}_2\text{O}$, 50 mol of alcohol (iso-butanol) is needed.

From the calculation as shown above, 0.05052 mol of $\text{VOPO}_4 \cdot 2\text{H}_2\text{O}$ is used.

$$\frac{0.05052 \text{ mol VOPO}_4 \cdot 2\text{H}_2\text{O}}{1 \text{ mol VOPO}_4 \cdot 2\text{H}_2\text{O}} \times 50 \text{ mol alcohol} = 2.5260 \text{ mol alcohol}$$

Thus, 2.5260 mol of alcohol (iso-butanol) is needed for 0.05052 mol of $\text{VOPO}_4 \cdot 2\text{H}_2\text{O}$.

Molecular formula of iso-butanol = $\text{C}_4\text{H}_{10}\text{O}$

Molecular weight of Carbon = 12.011 g/mol

Molecular weight of Oxygen = 15.9994 g/mol

Molecular weight of Hydrogen = 1.0079 g/mol

Molecular weight of $\text{C}_4\text{H}_{10}\text{O}$ = $(4 \times 12.011 \text{ g/mol}) + (10 \times 1.0079 \text{ g/mol})$
 $+ 15.9994 \text{ g/mol}$

= 74.1224 g/mol

Density of $\text{C}_4\text{H}_{10}\text{O}$ = 0.802 g/cm³ at 20 °C

Mass of $\text{C}_4\text{H}_{10}\text{O}$ = 74.1224 g/mol \times 2.5260 mol

= 187.2332 g

Density = $\frac{\text{mass}}{\text{volume}}$

Volume of iso-butanol = $\frac{\text{mass}}{\text{density}}$

= $\frac{187.2332 \text{ g}}{0.802 \text{ g/cm}^3}$

= 233.4578 cm³

Therefore, total volume of iso-butanol added is 233.4578 cm³.

APPENDIX B: Volume of Distilled Water Used

(24 ml H₂O/ g solid)

15 g of V₂O₅ is used as a starting material.

Thus, the volume of distilled water needed = 15 g × (24 ml H₂O/ g solid)
= 360 ml

APPENDIX C: Crystallite Size Measurements by using Powder XRD Technique

Crystallite size, T given by Debye-Scherrer equation: $T(\text{\AA}) = \frac{0.89\lambda}{FWHM \times \cos\theta}$

Given $\lambda_{\text{Cu K}\alpha} = 1.54\text{\AA}$

$$FWHM (\text{rad}) = FWHM (^{\circ}) \times \frac{\pi}{180^{\circ}}$$

APPENDIX D: Preparation of Diphenylamine, Ph₂NH Indicator (Redox Titration)

1 g of diphenylamine was weighed and dissolved in a few ml of concentrated sulphuric acid, H₂SO₄. Then the solution was transferred to a 100 ml volumetric flask and further top up with concentrated H₂SO₄.

APPENDIX E: Preparation of 2 M Sulphuric Acid, H₂SO₄ Solution

Concentrated H₂SO₄ (95- 98%)

$$1\text{L} = 1.84\text{ kg} = 1840\text{ g} / 1000\text{cm}^3 = 1.84\text{ g/cm}^3$$

$$\begin{aligned}\text{Molecular weight of H}_2\text{SO}_4 &= 2(1.00\text{ g/mol}) + 32.07\text{ g/mol} + 4(16.00\text{ g/mol}) \\ &= 98.07\text{ g/mol}\end{aligned}$$

$$\text{Concentration of 95- 98\% H}_2\text{SO}_4 = \frac{1.84\text{ g/cm}^3}{98.07\text{ g/mol}} \times \frac{95}{100} \times 1000 = 17.82\text{ M}$$

$$M_1 V_1 = M_2 V_2 \quad \text{where } M_1 = \text{concentration of 95- 98\% H}_2\text{SO}_4$$

$$M_2 = \text{concentration of diluted H}_2\text{SO}_4 (2\text{ M})$$

$$V_1 = \text{volume of 95- 98\% H}_2\text{SO}_4$$

$$V_2 = \text{volume of diluted H}_2\text{SO}_4 (2\text{ M})$$

$$(17.82\text{ M}) (V_1) = (2\text{ M}) (1000\text{ cm}^3)$$

$$V_1 = 112.23\text{ cm}^3$$

APPENDIX F: Preparation of 0.1 M Sulphuric Acid, H₂SO₄ Solution

$$M_1V_1 = M_2V_2$$

where M_1 = concentration of 95- 98% H₂SO₄

M_2 = concentration of diluted H₂SO₄ (0.1 M)

V_1 = volume of 95- 98% H₂SO₄

V_2 = volume of diluted H₂SO₄ (0.1 M)

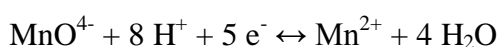
$$(17.82 \text{ M}) (V_1) = (0.1 \text{ M}) (1000 \text{ cm}^3)$$

$$V_1 = 5.61 \text{ cm}^3$$

APPENDIX G: Preparation of 0.01 M Potassium Permanganate, KMnO₄

(Redox Titration)

$$\text{Normality, } N (\text{eq/L}) = M (\text{mol/L}) \times n (\text{eq/mol})$$



$$\text{Molarity, } M (\text{mol/L}) = \frac{N(\text{eq/L})}{n(\text{eq/mol})}$$

$$= \frac{0.01}{5}$$

$$= 0.002 \text{ M}$$

$$\text{Molecular weight for KMnO}_4 = 39.10 \text{ g/mol} + 54.94 \text{ g/mol} + 4 (16.00 \text{ g/mol})$$

$$= 158.04 \text{ g/mol}$$

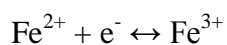
$$\text{Weight for KMnO}_4 \text{ in } 1000 \text{ cm}^3 \text{ diluted (0.1 M) H}_2\text{SO}_4 = 0.002 \times 158.04$$

$$= 0.3161 \text{ g}$$

APPENDIX H: Preparation of 0.01 M Ammonium Iron(II) Sulphate,

$(\text{NH}_4)_2\text{Fe}(\text{SO}_4)_2 \cdot 6\text{H}_2\text{O}$ (Redox Titration)

$$\text{Normality, } N (\text{eq/L}) = M (\text{mol/L}) \times n (\text{eq/mol})$$



$$\begin{aligned} \text{Molarity, } M (\text{mol/L}) &= \frac{N(\text{eq/L})}{n(\text{eq/mol})} \\ &= \frac{0.01}{1} \\ &= 0.01 \text{ M} \end{aligned}$$

$$\begin{aligned} \text{Molecular weight for } (\text{NH}_4)_2\text{Fe}(\text{SO}_4)_2 \cdot 6\text{H}_2\text{O} &= 2 (14.00 \text{ g/mol}) + 20 (1.00 \text{ g/mol}) \\ &\quad + 55.85 \text{ g/mol} + 2 (32.07 \text{ g/mol}) + \\ &\quad 14 (16.00 \text{ g/mol}) \\ &= 391.99 \text{ g/mol} \end{aligned}$$

$$\begin{aligned} \text{Weight for } (\text{NH}_4)_2\text{Fe}(\text{SO}_4)_2 \cdot 6\text{H}_2\text{O} \text{ in } 1000 \text{ cm}^3 \text{ diluted } (0.1 \text{ M}) \text{ H}_2\text{SO}_4 \\ &= 0.01 \times 392.14 \\ &= 3.9214 \text{ g} \end{aligned}$$

APPENDIX I: Oxidation State of Vanadium (Redox Titration)

Catalysts	V_{AV}	% of V^{4+}	% of V^{5+}
A	4.1241	87.59	12.41
B	4.2766	72.34	27.66
C	4.1111	88.89	11.11
D	4.1126	88.74	11.26

According to Niwa and Murakami (1982),

$$T_1 = V^{4+} + 2V^{3+} = 20 [MnO_4^-] V_1 \quad (1)$$

$$T_2 = V^{5+} + V^{4+} + V^{3+} = 20 [Fe^{2+}] V_2 \quad (2)$$

$$T_3 = V^{5+} = 20 [Fe^{2+}] V_3 \quad (3)$$

$$(2) - (3): \quad V^{3+} + V^{4+} = 20 [Fe^{2+}] V_2 - 20 [Fe^{2+}] V_3 \quad (4)$$

$$(1) - (4): \quad V^{3+} = 20 [MnO_4^-] V_1 - 20 [Fe^{2+}] V_2 + 20 [Fe^{2+}] V_3 \quad (5)$$

Substitute (5) into (1):

$$\begin{aligned} V^{4+} + 2(20 [MnO_4^-] V_1 - 20 [Fe^{2+}] V_2 + 20 [Fe^{2+}] V_3) &= 20 [MnO_4^-] V_1 \\ V^{4+} &= 20 [MnO_4^-] V_1 - 40 [MnO_4^-] V_1 + 40 [Fe^{2+}] V_2 - 40 [Fe^{2+}] V_3 \\ &= 40 [Fe^{2+}] V_2 - 40 [Fe^{2+}] V_3 - 20 [MnO_4^-] V_1 \end{aligned} \quad (6)$$

Substitute (5) and (6) into (2):

$$\begin{aligned} 20 [Fe^{2+}] V_2 &= V^{5+} + (40 [Fe^{2+}] V_2 - 40 [Fe^{2+}] V_3 - 20 [MnO_4^-] V_1) + (20 [MnO_4^-] V_1 \\ &\quad - 20 [Fe^{2+}] V_2 + 20 [Fe^{2+}] V_3) \\ V^{5+} &= 20 [Fe^{2+}] V_3 \end{aligned} \quad (7)$$

$$\begin{aligned}
 \text{From (5): } V^{3+} &= 20 (0.01) V_1 - 20 (0.01) V_2 + 20 (0.01) V_3 \\
 &= 0.2 (V_1 - V_2 + V_3)
 \end{aligned} \tag{8}$$

$$\begin{aligned}
 \text{From (6): } V^{4+} &= 40 (0.01) V_2 - 40 (0.01) V_3 - 20 (0.01) V_1 \\
 &= 0.4 V_2 - 0.4 V_3 - 0.2 V_1
 \end{aligned} \tag{9}$$

$$\begin{aligned}
 \text{From (7): } V^{5+} &= 20 (0.01) V_3 \\
 &= 0.2 V_3
 \end{aligned} \tag{10}$$

The average vanadium valence is calculated as:

$$V_{AV} = \frac{3V^{3+} + 4V^{4+} + 5V^{5+}}{V^{3+} + V^{4+} + V^{5+}} \tag{11}$$

VPO24:

$$V_1 = 10.15, V_2 = 11.10, V_3 = 1.33$$

$$\begin{aligned}
 \text{From (6): } V^{4+} &= 40 (0.01) V_2 - 40 (0.01) V_3 - 20 (0.01) V_1 \\
 &= 0.4 V_2 - 0.4 V_3 - 0.2 V_1 \\
 &= 0.4 (11.10) - 0.4 (1.33) - 0.2 (10.15) \\
 &= 1.878
 \end{aligned}$$

$$\begin{aligned}
 \text{From (7): } V^{5+} &= 20 (0.01) V_3 \\
 &= 0.2 V_3 \\
 &= 0.2 (1.33) \\
 &= 0.266
 \end{aligned}$$

The average vanadium valence is calculated as:

$$\begin{aligned}
 V_{AV} &= \frac{3V^{3+} + 4V^{4+} + 5V^{5+}}{V^{3+} + V^{4+} + V^{5+}} \\
 &= \frac{3(0) + 4(1.878) + 5(0.266)}{0 + 1.878 + 0.266} \\
 &= 4.1241
 \end{aligned}$$

If V_{AV} of VPO24 = 4.1241

$$V^{5+} (\%) = 12.41 \%$$

$$\begin{aligned}
 V^{4+} (\%) &= (100 - 12.41) \% \\
 &= 87.59 \%
 \end{aligned}$$

VPO48:

$$V_1 = 8.60, V_2 = 11.30, V_3 = 3.033$$

$$\begin{aligned}
 \text{From (6): } V^{4+} &= 40 (0.01) V_2 - 40 (0.01) V_3 - 20 (0.01) V_1 \\
 &= 0.4 V_2 - 0.4 V_3 - 0.2 V_1 \\
 &= 0.4 (11.30) - 0.4 (3.033) - 0.2 (8.60) \\
 &= 1.5868
 \end{aligned}$$

$$\begin{aligned}
 \text{From (7): } V^{5+} &= 20 (0.01) V_3 \\
 &= 0.2 V_3 \\
 &= 0.2 (3.033) \\
 &= 0.6066
 \end{aligned}$$

The average vanadium valence is calculated as:

$$\begin{aligned}
 V_{AV} &= \frac{3V^{3+} + 4V^{4+} + 5V^{5+}}{V^{3+} + V^{4+} + V^{5+}} \\
 &= \frac{3(0) + 4(1.5868) + 5(0.6066)}{0 + 1.5868 + 0.6066} \\
 &= 4.2766
 \end{aligned}$$

If V_{AV} of VPO48 = 4.2766

$$V^{5+} (\%) = 27.66 \%$$

$$V^{4+} (\%) = (100 - 27.66) \%$$

$$= 72.34 \%$$

VPO72:

$$V_1 = 11.30, V_2 = 12.15, V_3 = 1.30$$

$$\begin{aligned}
 \text{From (6): } V^{4+} &= 40 (0.01) V_2 - 40 (0.01) V_3 - 20 (0.01) V_1 \\
 &= 0.4 V_2 - 0.4 V_3 - 0.2 V_1 \\
 &= 0.4 (12.15) - 0.4 (1.30) - 0.2 (11.30) \\
 &= 2.08
 \end{aligned}$$

$$\begin{aligned}
 \text{From (7): } V^{5+} &= 20 (0.01) V_3 \\
 &= 0.2 V_3 \\
 &= 0.2 (1.30) \\
 &= 0.26
 \end{aligned}$$

The average vanadium valence is calculated as:

$$\begin{aligned}
 V_{AV} &= \frac{3V^{3+} + 4V^{4+} + 5V^{5+}}{V^{3+} + V^{4+} + V^{5+}} \\
 &= \frac{3(0) + 4(2.08) + 5(0.26)}{0 + 2.08 + 0.26} \\
 &= 4.1111
 \end{aligned}$$

If V_{AV} of VPO72 = 4.1111

$$V^{5+} (\%) = 11.11 \%$$

$$V^{4+} (\%) = (100 - 11.11) \%$$

$$= 88.89 \%$$

VPO96:

$$V_1 = 10.85, V_2 = 11.85, V_3 = 1.30$$

$$\begin{aligned}
 \text{From (6): } V^{4+} &= 40 (0.01) V_2 - 40 (0.01) V_3 - 20 (0.01) V_1 \\
 &= 0.4 V_2 - 0.4 V_3 - 0.2 V_1 \\
 &= 0.4 (11.85) - 0.4 (1.30) - 0.2 (10.85) \\
 &= 2.05
 \end{aligned}$$

$$\begin{aligned}
 \text{From (7): } V^{5+} &= 20 (0.01) V_3 \\
 &= 0.2 V_3 \\
 &= 0.2 (1.30) \\
 &= 0.26
 \end{aligned}$$

The average vanadium valence is calculated as:

$$\begin{aligned}
 V_{AV} &= \frac{3V^{3+} + 4V^{4+} + 5V^{5+}}{V^{3+} + V^{4+} + V^{5+}} \\
 &= \frac{3(0) + 4(2.05) + 5(0.26)}{0 + 2.05 + 0.26} \\
 &= 4.1126
 \end{aligned}$$

If V_{AV} of VPO96 = 4.1126

$$V^{5+} (\%) = 11.26 \%$$

$$V^{4+} (\%) = (100 - 11.26) \%$$

$$= 88.74 \%$$